Hindawi
International Journal of Photoenergy
Volume 2023, Article ID 3801813, 35 pages
https://doi.org/10.1155/2023/3801813

Review Article

A Review of the Technological Advances in the Design of Highly Efficient Perovskite Solar Cells

George G. Njema and Joshua K. Kibet

Department of Chemistry, Egerton University, Njoro, Kenya

Correspondence should be addressed to Joshua K. Kibet; jkibet@egerton.ac.ke

Received 6 February 2023; Revised 24 March 2023; Accepted 10 July 2023; Published 7 August 2023

Academic Editor: Daniel T. Cotfas

The search for renewable and sustainable energy for energy security and better environmental protection against hazardous emissions from petro-based fuels has gained significant momentum in the last decade. Towards this end, energy from the sun has proven to be reliable and inexhaustible. Therefore, better light harvesting technologies have to be sought. Herein, the current trends in the development of perovskite solar cells with a focus on device engineering, band alignment, device fabrication with superior light harvesting properties, and numerical simulation of solar cell architectures are critically reviewed. This work will form the basis for future scientist to have a better scientific background on the design of highly efficient solar cell devices, which are cost-effective to fabricate, highly stable, and eco-friendly. This review presents thorough essential information on perovskite solar cell technology and tracks methodically their technological performance overtime. The photovoltaic (PV) technology can help to reduce pollution related to greenhouse gas emissions, criterion pollutant emissions, and emissions from heavy metals and radioactive species by nearly 90%. Following the introduction of highly efficient perovskite solar cell (PSC) technologies, the problems associated with stability, short life-time and lead-based perovskite solar cell configurations have significantly been minimized. The fabrication and simulation of perovskite solar cells has been made possible with advanced technologies and state-of-the-art computational codes. Furthermore, device simulation strategies have lately been used to understand, select appropriate materials, and gain insights into solar cell devices' physical behavior in order to improve their performances. Numerical simulation softwares such as the 1-dimenional solar cell capacitance simulator (SCAPS-1D), Silvaco ATLAS, and wx-analysis of microelectronic and photonic structures (wxAMPS) used to understand the device engineering of solar cells are critically discussed. Because of the need to produce charge collection selectivity, hole transport materials (HTMs) as well as electron transport materials (ETMs) constitute essential PSC components. In this work, the synthesis of inorganic HTMs, as well as their characteristics and uses in various PSCs comprising mesoporous and planar designs, are explored in detail. It is anticipated that the performance of inorganic HTLs on PSCs would encourage further research which will have a significant influence on the future designs and fabrication of highly efficient solar cells.

1. Introduction

The consistent rise in the advancement of technology, global warming, and enhanced living standards globally is a precursor in the search for clean, secure, and reliable energy resources. Accordingly, traditional fossil fuel energy sources are insufficient to support the sustainable growth of human society and environmental protection [1]. For many years, humans have been using environmentally degrading energy sources which have led to climate changes, global warming, and public health problems. Therefore, rigorous scientific research has gained immense traction in order to identify a sustainable renewable energy. Of the many alternative sources of energy such as biofuels, geothermal energy, wind energy, and nuclear energy, solar energy is one of the most feasible, reliable, and inexhaustible resource. Generally, a solar cell is a device that uses photovoltaic effects or photochemical reactions to transform light energy directly into electrical energy [2]. In recent years, perovskite solar cells have attracted enormous attention because of their remarkable photovoltaic performance. The general formula of PSCs is ABX_3 where A is a monovalent cation such as cesium or

potassium, B is a divalent cation, and X is a halogen anion. The perovskite materials are regarded as one of the preeminent materials for the next generation of photovoltaic technology because of their distinctive properties, including high electron mobility (800 cm^2/Vs), high carrier diffusion length (greater than 1 m), and electrical properties charge transport behavior [3]. High transport excitons are what distinguish organic absorbers from inorganic photoactive materials [4].

The primary drawback towards the development of large-scale production of solar energy generation is its high cost, although in the recent century, the cost of manufacturing conventional silicon-based solar device has decreased from $76.67/W in 1977 to as low as $0.36/W in 2022 [5]. Nevertheless, the cost of fabricating such a solar device is about 10-20 times higher than that of energy obtained through fossil fuels. Perovskite is the promising photovoltaic technology capable of replacing the conventional silicon solar cells and offers robust competition against other emerging solar technologies such as dye-sensitized solar cells [6]. PSCs are an efficient newcomer solar cell technology with enormous commercial alternatives of fulfilling the global energy demands. Unlike the conventional fossil fuels, PSCs convert inexhaustible solar photons in a pollution-free manner [7, 8]. According to Guo et al. [9], PSCs have made an incredible progress in terms of their power conversion efficiencies (PCE), reaching a practical value of over 31.01% in approximately 10 years [5], whereas the conventional silicon solar cells reached 26% after four decades of active research but with serious problems of short-lifetime, instability, high production costs, recombination, reflection, and absorption losses, as well as efficiency problems [10, 11]. On the other hand, a power conversion efficiency (PCE) of 20% has been attained in solution-processed perovskite-based solar cells [12].

The attractive features of PCS include their brilliant photovoltaic performance and cheap processing techniques. PSC scans can easily be synthesized using simple local techniques such as screen printing, spin coating, dual source evaporation techniques, and dip coating [13]. In order to overcome the Shockley-Quisser limit of 35.5% in PSCs, tandem perovskite solar cells have been advanced [14]. Besides, PSCs are environmentally sustainable when converting incident solar energy into electricity. Perovskite solar cells have the potential to contribute to sustainable development goals such as increasing the production of clean energy (SDG 7) and climate action (SDG 13) [15]. The potential use of perovskite materials in solar cells is contributed by device stability and its remarkable efficiency. A mineral calcium titanium oxide, the very first perovskite crystal to be identified, has the same crystal structure as a material known as a perovskite. The chemical formula for perovskite compounds is typically ABX_3, where "A" and "B" stand for cations and "X" is an anion which bonds to both of them [16, 17]. Perovskite structures can be created by combining a variety of various components. This compositional versatility allows researchers to design perovskite crystals with a broad range of physical, optical, and electrical properties. Figure 1 shows a representation of a lead-based perovskite.

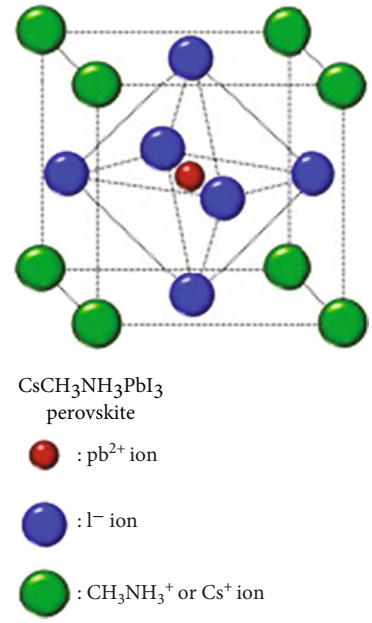

Figure 1: Structural composition of a lead-based methylammonium perovskite [18].

Today, perovskite crystals can be found in solar cells, memory chips, and ultrasound devices. The basic structure of perovskite solar cells consists of an electron transport layer (ETL) and a hole transport layer (HTL) where the free electrons and holes get injected into. Usually, the anode and cathode in a perovskite solar cell structure are fabricated using fluorine-doped tin oxide (FTO), indium gallium zinc oxide (IGZO) glass materials, and a metal back contact. Currently, p-type or n-type silicon is utilized most frequently for cell architectures, and efficiency is determined either by busbar configuration, junction, or passivation type [19]. Theoretically, contact grids are placed on the rear of the cell rather than the front to avoid shading losses; interdigitated back contact (IBC) solar cells potentially reach better efficiencies. IBC cells, which can achieve efficiencies of 20–22%, use high-purity n-type silicon. Panels using advanced heterojunction (HJT) cells, n-type tunnel oxide passivated interface (TOPcon), and monocrystalline silicon passivated emitter and rear contact (PERC) cells can attain efficiencies in excess of 21% [20]. Tandem silicon-perovskite solar cells have been reported to reach theoretical limits of 43% and have demonstrated efficiency exceeding 30% in testing, although they are still mostly in the development stages and are not yet widely available in the market [21]. Nonetheless, efficiencies can be affected by a number of other variables such as temperature, shade, panel orientation, and irradiance at the installation site. The largest electricity output can be attained and increased by optimizing the overall efficiency of the solar cell installation [22].

2. Lead-Based Perovskite Solar Cells

As a visible light sensitizer, a perovskite structure with a 3.8% photoelectric conversion efficiency (PCE) based on

methylammonium lead bromide ($CH_3NH_3PbBr_3$) and methylammonium lead iodide ($CH_3NH_3PbI_3$) have been utilized previously [23, 24]. Researchers were drawn to PSCs mostly in the field of photoelectric conversion because of their low cost and simple production procedure. In 2019, the PCE of PSCs rose from 3.8% to as high as 25.2% in 2020 [25]. Lead-based perovskite solar cells appear to have nearly ideal optical and electrical characteristics. Lead-based perovskite solar cells recently outperformed solar cells based on Cu(In,Ga)(S,Se)$_2$, CdTe, and Si, reaching an efficiency of 23.7%. However, there are two drawbacks with Pb-based perovskite solar cells: poor stability and severe toxicity [26]. For each parameter, optimization is carried out to obtain the highest PCE. Due to its exceptional characteristics, including an optimal band gap, a wide absorption spectrum, a good carrier transport system, ease of fabrication on a flexible substrate, a configurable band gap, and a long diffusion length, $CH_3NH_3PbI_3$ has become a good light harvester [27]. A typical $CH_3NH_3PbI_3$-based solar cell comprises a p-type (PEDOT: PSS) electrode at the top and n-type (PCBM) electrode at the bottom, as presented in Figure 2 [27, 28]. It has been previously reported that the best-performing planar cell using SnO_2 electron transport layer (ETL) has reached an average efficiency of 16.02% obtained from efficiencies measured from both reverse and forward voltage scans, as shown in Figure 2. The outstanding performance of SnO_2 ETLs is attributed to the excellent properties of nanocrystalline SnO_2 films, such as good anti-reflection, suitable band edge positions, and high electron mobility [28].

At first, the highest practical PCE of perovskite solar cells based on $CH_3NH_3PbI_3$ was 3.8% [29, 30], but more recently, the PCE of perovskite solar cells has reached 22.1% due to innovative fabrication procedures, better band alignment, and robust cell architectures [31, 32]. Materials for methylammonium lead halide perovskite are widely available and may be processed through low-cost production approaches. Because of the growing use of photovoltaics, lead has been employed extensively in the solar cell industry, posing serious environmental and occupational health hazards. When solar cell panels, particularly those made of perovskite solar cells, are broken, lead may leak into the environment and contaminate the air, soil, and groundwater [33]. Leaching and movement of toxic elements such as Pb from lead-based perovskite solar cells (PSCs) through water, air, and soil may cause etiological risks to both animals and plants.

2.1. Lead-Free Perovskites. Despite the fact that lead is permitted in solar modules, it would be ideal to find substitutes that preserve the distinct optoelectronic characteristics of lead halide perovskites. Previous studies has proven that less toxic ions like Sn^{2+}, Bi^{3+}, Ge^{2+}, Sb^{3+}, Mn^{2+}, and Cu^{2+} could be used as an alternative replacements to Pb^{2+} in perovskites to engineer new lead-free perovskite solar cells [34, 35]. The introduction of these metal cations not only increases the diversity of perovskite species but also enhances environmentally friendly features of PSCs [35]. For Sn-based PSCs, this type of material has a relatively high absorption coefficient estimated at $1.80 \times 10^4\,cm^{-1}$, but the oxidation of

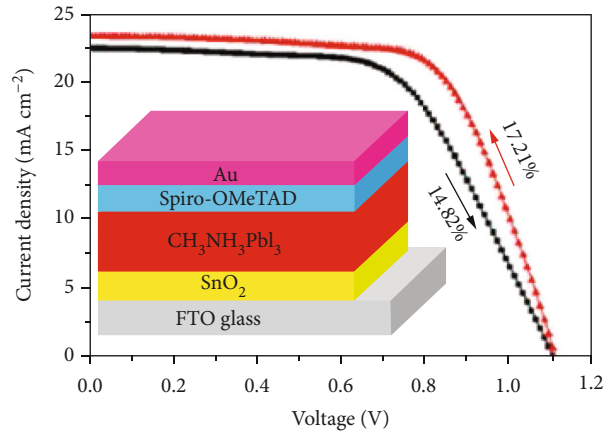

Figure 2: Device architecture of a lead halide perovskite solar cell based on SnO_2 ETL, where the red line is the reverse scan while the black line is the forward scan [28].

Sn^{2+} to Sn^{4+} is considered the main challenge limiting the advancement of Sn-based PSCs [35]. Numerous approaches have been advanced to prevent the oxidation of Sn in order to enhance its performance, but its chemical stability has become difficult to manage [35]. A variety of non- or low-toxic perovskite materials have been used for the development of environmentally friendly lead-free perovskite solar cells, some of which show excellent optoelectronic properties and device performances [36]. Tin appears to be an essential replacement to lead in order to minimize lead poisoning. Since lead may enter the human body, bind with enzymes, and get stored in soft tissues such as the spleen, kidney, liver, and the brain through blood circulation, lead poisoning eventually manifests as functional abnormalities in the neurological, digestive, and circulatory systems of the victim [37]. Typically, lead poisoning symptoms appear in most people when exposure reaches 0.5 mg/day [38]. A thorough examination of each of the Sn-based perovskites' fundamental physical characteristics as well as a comparison to those of the Pb-based perovskites shows a close similarity. Therefore, these materials ought to be able to equal the efficiency of the $APbI_3$ systems [39]. Towards this end, all inorganic, lead-free and organic-inorganic hybrid, and lead-free perovskite solar cells have proven reliable and cost-effective.

Double perovskites with the formula $A_2M + M_3 + X_6$ have been sought after in addition to the directly similar Sn- and Ge-based perovskites. These 3D materials have wider band gaps of about 2 eV and are typically more stable in air, although they have indirect band gaps, parity-forbidden transitions, 0D electronic dimensionality, large hole/electron effective masses, and indirect band gaps, which results in low exciton nobilities as well as poor carrier transport. Bismuth-based double perovskite solar cells share similarities with Cs_2SnI_6-based solar cells, but they have not yet attained high J_{sc} and PCE [39]. Previously, the efficiency of tin-based perovskite solar cells decreased largely with increased cell area because of the inhomogeneity of the tin perovskite films formed by a one-step deposition method; however, this setback has been solved by the two-

step deposition approach using appropriate solvents in order to enhance uniformity and improve the cell performance [40]. At present, more new lead-free perovskite materials with tunable optical and electrical properties are urgently required to design highly efficient and stable lead-free perovskite solar cells.

2.1.1. Lead-Free Double Perovskite Solar Cells. In the recent past, metal halide perovskites have attracted interest as semiconductor devices that achieve desirable properties for optoelectronic application; however, two major challenges—instability and the toxic nature of Pb—remain unaddressed [41]. For this reason, lead-free double perovskites (LFDPs) are emerging as the preferred photoactive absorbers because of their promising PV properties such as intrinsic chemical stability, in addition to being environmentally friendly [42]. Lead-free halide double perovskite nanocrystals are considered as one of the most promising alternatives to the lead halide perovskite nanocrystals because of their exceptional characteristics of nontoxicity, robust intrinsic thermodynamic stability, and rich and tunable optoelectronic properties [43]. Recently, lead-free double perovskites have redefined photovoltaic research, despite the fact that a detailed study of their optical, excitonic, and transport characteristics is yet to be understood [44, 45]. Studies by Jain et al. have shown that, in comparison to a pristine LFDP, alloyed versions of LFDPs have a longer exciton lifetime, suggesting a lower electron–hole recombination, which also leads to a higher quantum yield and better power conversion efficiency in the alloyed compounds [45]. Inorganic halide double perovskites show good stability because of their inorganic counterions [46]. LFDPs are therefore remarkable photoactive layers for optimal solar harvesting because they exhibit an increase in hole and electron mobilities [45, 47]. Double perovskites have gained importance due to their similar characteristics to lead halide perovskites and have been found to exhibit interesting optical and morphological properties [46]. Nonetheless, LFDPs have been found to suffer various drawbacks; low photoluminescence quantum yields, preparation of double perovskites needs high temperature which causes significant challenges in device fabrication, and tuning the morphology of double perovskite is quite difficult. Despite these obstacles, double perovskites have gained considerable research momentum recently and have established themselves as promising superstar alternatives to lead halide perovskites [46].

Currently, the LFDP structure, $Cs_2AgBiBr_6$, is receiving a lot of interest as a light-harvesting device in PSCs [48]. Numerical simulation of the device configuration, FTO/SnO_2/$Cs_2AgBiBr_6$/P_3HT/Au, based on SCAPS-1D gave a low PCE of 1.81% [48]. This was attributed to the unsuitable band alignment of P_3HT'Au with the perovskite, its poor carrier mobility, and extensive charge recombination [49]. By changing the absorber's defect density value from $1 \times 10^{13}\,cm^{-3}$ to $1 \times 10^{19}\,cm^{-3}$ for the most effective device, the impact of the defect was evaluated with $CuSbS_2$ as the HTL [48]. Furthermore, by optimizing the double-perovskite layer thickness, which was found to be 400 nm, the device's photovoltaic performance was further enhanced, and this resulted to a PCE of 18.18% while operating at peak efficiency [50]. The optimized V_{oc} was 1.39 V, J_{sc} was 16.04 mA/cm^2, and the FF was 78.34%, which shows that the double-perovskite absorber layer ($Cs_2AgBi_{0.75}Sb_{0.25}Br_6$) is a suitable candidate for the design of a highly effective Pb-free DPSC [50]. Figure 3 presents an enhanced LFDP solar cell architecture.

Tin is a key component of lead-free PSCs because it has a similar diameter and valence as lead. This leads researchers to replace lead with tin in order to create $ASnX_3$ perovskite films [51]. However, compared to a lead-based perovskite solar cell, the tin-based device's greatest PCE was just 6.4% [52, 53]. More crucially, the material's unstable Sn^{2+} ion is easily converted into $Sn^{4+,}$ which diminishes the photovoltaic performance [54]. In tin-based perovskite, a strong correlation exists between the Lewis base molecules' molecular hardness and how well they passivate [51]. By triggering charge redistribution and saturating the dangling states while at the same time decreasing the quantities of deep band gap states, it is demonstrated how the level of hardness of the Lewis adsorbate controls the stabilization of the PV device [51]. The first effect is to change the tin vacancy's (VSn) stubborn spatial distribution. New lead-free perovskites with good intrinsic stability for solar applications are still challenging to design [53].

2.2. Organic-Inorganic Hybrid Solar Cell. Organic and inorganic hybrid lead halide perovskites have successfully emerged as revolutionary optoelectronic semiconductors for use in various device applications. The long-term stability and lead toxicity of hybrid lead halide perovskites have gained traction; therefore, all-inorganic lead-free perovskites have become an alternative perovskite for use in solar cell and optoelectronic applications [55]. Halide perovskites are produced using cheap ingredients that work with very effective deposition techniques previously employed for organic electronics [56, 57]. In order to make use of the low-cost cell manufacture of organic photovoltaics (OPV) and to gain additional benefits from the inorganic component such as tunable absorption spectra, hybrid solar cells incorporate organic, and inorganic components. Organic-inorganic hybrid perovskite solar cells (PSCs) have recently attracted a lot of interest in the photovoltaic community, but recent research has indicated that a missing hydrogen occasioned by poor stability can cause massive energy losses and may therefore be unreliable in the long run [44]. High solar efficiency of more than 25% has been demonstrated by hybrid organic-inorganic perovskite-based solar cells [58]. Accordingly, the presence of organic molecules in the material that contain carbon and hydrogen is essential for obtaining remarkable photovoltaic performance since these molecules are thought to suppress energy-draining "nonradiative recombination" occurrences. Even though hybrid solar cells have the capacity to produce high power conversion efficiencies (PCE), the efficiencies currently attained are modest [59]. Although the power conversion efficiencies now attained by hybrid solar cells are rather low, they have the potential to reach higher PCEs. The electrical structure of the inorganic substance utilized as an electron acceptor in hybrid solar cells, in particular, has a critical role in the device's performance. An inorganic acceptor has an ideal electrical structural design. Four main

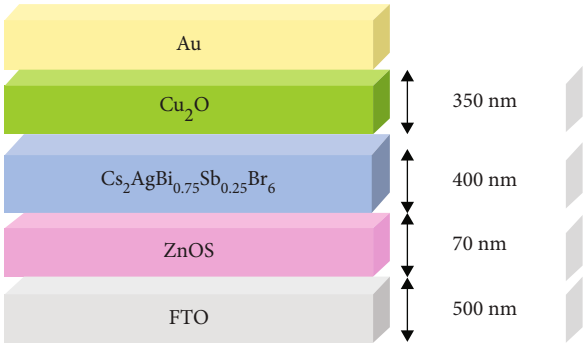

Figure 3: Enhanced double perovskite solar cells without lead [50].

categories of materials have been studied: silicon, metal oxide nanoparticle, narrow band gap nanoparticle, and cadmium compounds which previously gave a PCE of 4% [60]. In inorganic-organic hybrid heterojunction solar cells, organometallic halide perovskites have the ability to function both as a hole conductor and as a light harvester. A 15% power conversion efficiency is provided by the sequential deposition as observed in Figure 4 [26]. Whereas organic–inorganic tin halide perovskites have shown good semiconducting characteristic, the instability of tin in its 2+ oxidation state has exhibited an overwhelming challenge [34].

Because of their high power conversion efficiency and lack of emissions, photovoltaics are thought to be a possible solution to the problems facing renewable energy advancement and clean environment. However, two significant limitations for high-performance solar cells are the restricted spectral absorption range and strong recombination events at electrode/electrolyte interfaces in addition to nonradiative and charge transport losses [60, 62]. In order to make use of the low-cost cell manufacture of organic photovoltaics (OPV) and to gain additional benefits from the inorganic component, such as tuneable absorption spectra, solar hybrid cells combine organic and inorganic components. Even though hybrid solar cells have the capacity to produce higher power conversion efficiencies (PCE), the efficiencies currently attained are modest. The electrical structure of the inorganic substance utilized as electron acceptor for hybrid solar cells, in particular, has a critical role in the device's performance. An inorganic acceptor has an ideal electrical structural design [60]. Investigated material types include silicon, metal oxide nanoparticles, narrow band gap nanoparticles, and cadmium compounds. The state-of-the-art at the moment is cadmium sulphide (CdS) quantum dots which provide a practical PCE of more than 4% [60, 63].

2.3. Tandem Perovskite Solar Cells. Perovskite-based tandem solar cells (TSCs) are an emerging PV technology with the potential to surpass the S–Q theoretical limit of efficiency of single-junction silicon solar cells, which have the capacity to achieve efficiencies of approximately 45% through complete optimization of the optical and electrical parameters [64]. Through the use of tandem strategy, high efficiency of up to 29% has been achieved [65]. Silicon solar cells have a theoretical bandgap of 1.2 eV, and this implies that the PCE is 32% [66]. Both physically stacking 4-terminal (4-T) and monolithically series integration 2-terminal (2-T) subcells can be used to create perovskite-perovskite tandems [67]. A 2-T arrangement necessitates accurate bandgap matching due to the requirement for current matching, but a 4-T arrangement is mostly dependent on the effectiveness of individual subcells and somewhat resistant to band gap (Eg) identification. However, the 2-T arrangement is favored over the 4-T because it has less parasitic absorption, more practical, and has superior economic characteristics [68]. With regard to hybrid perovskite, a 2-T structure with the ideal Eg ratio of 1.2 and 1.8 eV can theoretically provide a PCE of about 36% [69]. Therefore, improving 2-T perovskite tandems seems to be a fascinating scientific challenge that will encourage the creation of additional hybrid perovskite and reduce the cost of PV to encourage technology transfer [70]. Examples of perovskite-perovskite tandem device is presented in Figure 5. The power conversion efficiency (PCE) of perovskite/perovskite tandem solar cells has surpassed that of single-junction perovskite solar cells [71].

The highest-quality perovskite solar cell may achieve a PCE of more than 31%. Researchers can produce perovskite with a close band gap to the ideal one by manipulating the chemical composition of the perovskite crystal [70]. Engineering multilayered perovskite solar cells, where the layers should have varied band gaps, is another way to approach the optimum band gap [65]. Due to the presence of many layers, most of the sun's total power is converted to electricity when low-energy photons stimulate electrons in layers with a smaller band gap and high-energy photons stimulate electrons in layers with a wider band gap [72]. The conversion efficiency of 26% has been attained by using multiple junction perovskite solar cells with different band gap sizes [73]. Moreover, in a "tandem cell" arrangement with silicon cells, a tunable layer of perovskite can be added to collect photons, thus improving the power conversion efficiency [74].

2.4. All-Inorganic Perovskite Solar Cells. Due to their exceptional thermal and environmental stability, all-inorganic perovskite materials have been rapidly made by employing pure inorganic cations that can substitute the A-site organic cations in the ABX_3 structure. All-inorganic perovskite solar cells (I-PSCs) have currently reached efficiency levels of 19% and have a wide range of potential applications [75]. Perovskites made entirely of inorganic $CsPbI_3$ have a lot of potential for use in tandem solar cells and other photovoltaic combinations. Nonetheless, $CsPbI_3$ perovskite solar cells (PSCs) continue to face a lot of obstacles which cause them to have a lower PCE as compared to the organic-inorganic PSCs counterparts [76]. Figure 6 shows an example of an all-inorganic PSC architecture.

Due to their exceptional qualities, such as a tunable bandgap, remarkable defect tolerance, prolonged exciton diffusion range, high carrier mobility, and absorption coefficient, organometallic lead halide perovskites are potential material for solar cells [77]. Organometallic lead halide PSCs have so far shown outstanding power conversion efficiency, reaching up to 25.2% [77]. However, their operational lifetimes are constrained as a result of the organic components'

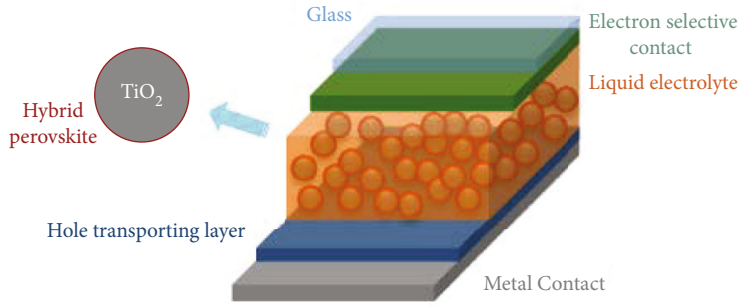

Figure 4: Device architecture of an organic-inorganic hybrid solar cell [61].

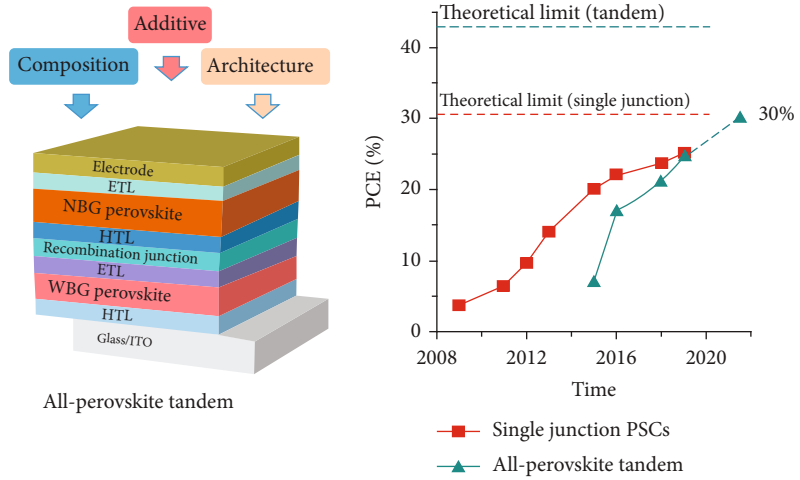

Figure 5: The perovskite cell architecture and power conversion efficiency of perovskite (red line) and perovskite tandem (green line) solar cells [67].

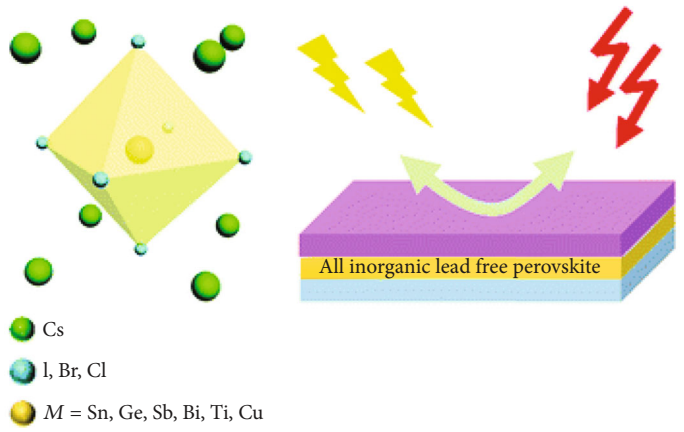

Figure 6: An example of an all-inorganic perovskite solar cell configuration [55].

susceptibility to environmental degradation. Consequently, scientists are particularly interested in all-inorganic perovskite, particularly cesium lead triiodide ($CsPbI_3$), which has higher chemical and compositional stability. However, the major drawback to these materials is its phase instability in the black phase and the poisonous nature of lead [77].

As a brief overview, the scientific community has given the hybrid organometallic trihalide perovskite ($CH_3NH_3SnI_3$) significant attention since it was reported in the literature [78, 79]. It has excellent photoelectric properties and is simple to process in solutions. It has a direct band gap of 1.55 eV, a weak binding energy of approximately 0.03 eV, an absorption coefficient greater than 104 cm^{-1}, and a small difference between the band gap potential and the device's open-circuit voltage (Voc) [80]. Using the iodide $HC(NH2)^{2-}$ (SnI_3:$FASnI_3$)-based PSC, the effect on defect density, layer thickness, and doping

concentration has been investigated using the 1-dimensional solar cell capacitance simulator (SCAPS-1D) numerical code and found that the $V_{oc} = 0.92$ V, $J_{sc} = 22.65$ mA/cm^2, and FF = 67.74%, and an optimal PCE of 14.03% was achieved [81].

Lakhdar and Hima [82] reported the highest PCE of 18.16% based on $CH_3NH_3PbI_3$ solar cell and 9.56% with $CH_3NH_3SnI_3$ solar cell using Silvaco ATLAS simulation software [83]. Hima et al. [84] investigated the impact of the absorber layer thickness, charge mobility, and defect density on planar PSC with an efficiency of over 20% using analysis of microelectronic and photonic structures (AMPS-1D) [83]. Perovskite solar cells made of sheets of gallium-doped zinc oxide (GZO) have been designed, and a maximum theoretical PCE of 21.24% has been obtained [85, 86]. This is attributed to better carrier concentration of the photogenerated excitons.

2.5. Quantum Dot Solar Cells. A promising low-cost alternative to the current photovoltaic technologies such as crystalline silicon and thin inorganic films is the quantum-dot-sensitized solar cells (QDSCs). Quantum dots (QDs) could be made using low-cost techniques, and their size can be adjusted to customize their absorption spectrum [87]. To fabricate electron conductor/QD monolayer/hole conductor junctions with high optical absorbance, conventional dye-sensitized solar cells (DSCs) are used as a source of nanostructures exhibiting high microscopic surface area, redox electrolytes, and solid-state hole conductors [88]. A size-dependent absorption spectrum is produced by the quantum confinement of the exciton in the absorber material, which is a frequent characteristic of QD-based solar cells [89]. A wide-bandgap material's nanostructure that has been sensitized with a QD monolayer serves as the foundation of QDSCs [90, 91]. Theoretically, the QDSC can achieve a theoretical PCE of up to 66% due to the occurrence of a unique phenomenon called multiexciton production [92]. This makes QDSC a potential third-generation solar cell multiexciton generation (MEG) [92]. The experimental values of PCE for QDSCs are quite low compared to what is theoretically predicted. Hybridization of electron-hole pairs in the quasi-neutral zone is one possible cause of the observed low PCE. The proper choice of HTL and a suitable ETL is critical in reducing recombination losses and increasing QDSC efficiency [92, 93]. When, for instance, lead sulfide (PbS-TBAI) coated with tetrabutylammonium iodide is employed as the active layer, with tungsten trioxide (WO_3) is used as the ETL, a PCE of 15.51% is achieved [92].

The lowest constrained states of QDs will establish the effective band gap for absorption; for instance, the phenomenon of resonant tunneling can be used to increase the internal quantum efficiency for the gathering of charge carriers photoexcited in the QD [94]. A well-known stacking method in the Stranski-Krastanov growth mode can be used to create high-density QD arrays [95]. The vertical alignment of QDs is brought about by strain fields from the bottom QD layer that have extended into the barrier material. Electronic states can take on a wire-like appearance because of the strong vertical coupling among QDs. As a consequence, channeling the electrons and holes through the coupling between aligned QDs can result in elevated internal quantum efficiency for the collection of carriers photoexcited in the QDs. This phenomenon makes it possible to efficiently separate and inject the generated holes and electrons in QDs into the nearby p and n regions [96].

One can adjust the size and form of the InAs islands and subsequently the quantized levels of energy in order to control the absorption of the light spectrum by adjusting the deposition mode, the thickness of the intermediate layer, and the number of times the island layer is repeated. Figure 7 is a typical example of a quantum dot solar cell design. An essential approach to enhance the oxidation resistance of PbX QDs is through passivation of their surface via halides, a process which relies on the binding of halide ions to the Pb atoms on the surface and accordingly reduces the number of sites where O_2 can adsorb [98].

2.6. Lead Colloidal Quantum Dot Solar Cells. One of the most desirable QDs for creating innovative optoelectronic devices like solar cells, photodetectors, and biological labels is the lead sulphide (PbS) colloidal quantum dot solar cell [99]. PbS colloidal QDs have received significant interest as promising building blocks for optoelectronic devices because of their size-dependent band gap and tunability of electronic properties by means of surface chemistry and solution processability [100]. Finding a suitable approach to obtain high-quality QDs in a broad size range using less expensive, toxic-free, and eco-friendly precursors is challenging. Due to their easy solution processing, low material cost, long-term air stability, and potential for customizing their optoelectronic properties by adjusting size, composition, and surface chemistry, PbS colloidal QDs are appealing materials for the next-generation photovoltaic devices [101]. However, after solidification, the lengthy aliphatic ligands that commonly surround PbS QDs in solution function as barriers to charge transfer and transport between nearby QDs [102]. The ligand-exchange method, which is employed to remove such lengthy ligands, can produce a variety of surface traps including vacancies and dangling bonds. Recombination will significantly lower the performance of the device. Nonetheless, surface passivation techniques have been developed, and PbS quantum dot photovoltaics (QDPVs) have witnessed a considerable increase in PCE of over 10% [103]. However, the achieved PCE is still much lower than what is anticipated, and surface traps continue to be a major limiting factor for PbS QDPVs. The primary goals of the work on Schottky solar cells' performance improvement are to enhance metal species, create ligand strategies, and expand responses into the infrared spectrum [104]. In Schottky solar cells, ternary PbSxSe1x CQDs were used, and they performed better than PbS or PbSe CQDs. Choi et al. modified the PbS CQD/metal contact by adding an incredibly thin oxidized contact layer in order to enhance the Schottky barrier's quality and the functionality of the device [104]. A PbS CQD sheet was sandwiched between a material with a low work function and a high work function metal anode in an inverted Schottky CQD solar cell, and the best device was produced with a PCE of 3.8% and a record of 0.75 V [105, 106]. An example of a lead-based colloidal quantum dot is presented in Figure 8.

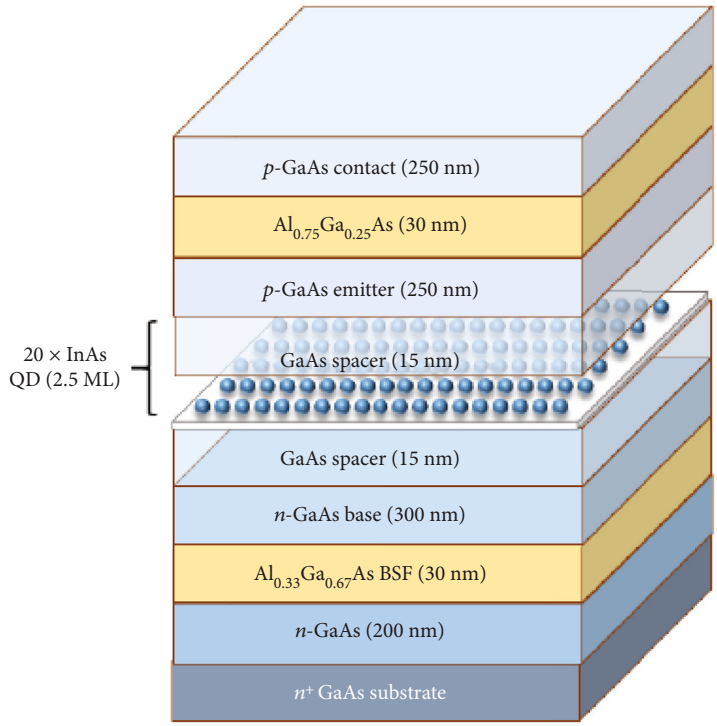

Figure 7: The quantum dot solar cell structure is depicted schematically and is made up of 20 InAs repeats [97].

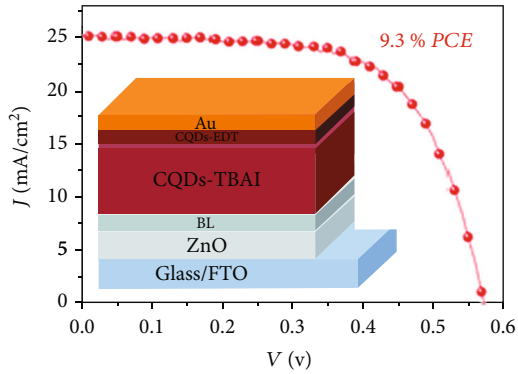

Figure 8: PbS colloidal quantum dot solar cell showing I-V characteristics and PCE [107].

3. Stability of All-Inorganic Perovskite Solar Cells

Due to their outstanding compatibilities with tandem devices, high carrier mobility, and strong thermal stability, all-inorganic perovskite solar cells (PSCs) have received a lot of interest [108]. The power conversion efficiency with all PSCs has exceeded 19% because of extensive research of these devices and ongoing process development. The manufacture for long-term application of PSCs in the air environment, however, still presents significant difficulties due to the comparatively poor phase stability. Many researchers have suggested numerous approaches such as additive engineering, interface engineering, and the construction of all-inorganic perovskite quantum dot solar cells, to enhance the long-term stability of all-inorganic perovskite solar cells [109].

Inorganic cations like Cs^+, Rb^+, Sn^+, and K^+ have thus been suggested to be employed to make an all-inorganic perovskite, $CsPbX_3$ (X = halide), in order to address the challenges resulting from environmental deterioration [110]. Unlike organic-inorganic hybrid solar cells, this cation substitution attempts to increase the chemical and thermal stability. Currently, $CsPbI_3$, $CsPbI_2Br$, $CsPbIBr_2$, and $CsPbBr_3$ are the most widely used inorganic perovskite solar cells. A good choice of solar energy harvesting is the $CsPbI_3$ material, which has a significantly small band gap (Eg = 1.73 eV). Among inorganic solar cells, cesium lead halide perovskite solar cells display the highest efficiency [77]. To increase phase stability, adding some bromide ions to Cs-perovskite instead of iodide ions could result in $CsPbBr_3$. However, this material's high band gap (Eg = 2.25 eV) restricts light harvesting, which consequently lowers the efficiency of the cells [77].

In comparison to hybrid solar cells, inorganic perovskite solar cells are reported to be more stable [77]. In fact, some researchers have noted the remarkable stability of inorganic solar cells throughout over time with or without encapsulation. Inorganic perovskite solar cells, for instance, were noted to be good substitutes to the stability problem of hybrid PSCs, particularly to the moisture instability caused by the material's high-hygroscopicity characteristics. However, it has been shown that the most widely used inorganic lead halide perovskite, $CsPbI_3$, suffers from severe phase instability problems in ambient air [77, 111]. Even without encapsulation, the all-inorganic PSCs exhibit minimal performance degradation in humid air (90–95% relative

humidity, at 25 ˚C) for more than 3 months (2640 hours) and can withstand extremely low temperatures of up to –22˚C [112].

3.1. Perovskite Efficiencies and Band Gap Characteristics. One or more electrons are always present around the nucleus of every atom, and negatively charged electrons are drawn to positively charged nuclei. The number of electrons that each atom has determines how many atoms can form a molecule. Its shared electrons float about the molecule. The outer electrons of the atom for which they orbit are considered to be in its "valence band" [113]. When photons of light "bump" the outer electron of a semiconductor material to a high energy state, they force electrons away from the valence band to the conduction band of a molecule, thus producing an electric current. The band gap is defined as the smallest amount of energy required to move each electron from the valence band to the conduction band [114]. An electron becomes a charge carrier which flows through the material it is a part of, when it moves to the conduction band and is no longer tethered to the orbit of the molecule. For this reason, it can be employed in photovoltaic cells to transport electrical energy.

Different colors of light photons carry varying amounts of energy, which is measured in electron volts (eV). Visible light photons have energies ranging from 1.75 eV (intense red) to 3.1 eV (violet). At 1.34 eV, the bandgap of an ideal photovoltaic material, maximum visible light should transform electrons to charge carriers [114]. Power conversion efficiency measures how much solar energy can be transformed into electricity by a solar cell (PCE). It has been noted that among layers of positively and negatively modified materials with an optimal bandgap, better efficiencies are achieveable [115]. The S-Q limit is the name given to this optimal efficiency [116]. The implication of the S-Q limit is that there is no material with the ideal bandgap that can approach the S-Q limit. By absorbing light over a wider spectrum of wavelengths, multijunction (tandem) solar cells (TSCs), which are made up of several light absorbers with noticeably different band gaps, have a high potential to surpass the S-Q efficiency limit of a single junction solar cell. Due to their customizable band gaps, high PCE up to 25.2%, and simple manufacture, PSCs make excellent candidates for TSCs. Narrow band gap PSCs, dye-sensitized, organic, and quantum dot solar cells are just a few of the numerous solar cell types that can easily be combined with PSCs, resulting in high PCEs - commonly made using a low-temperature solution approach [117].

Crystalline silicon-based technologies nowadays control the PV market because of their low manufacturing costs and strong material and manufacturing process reliability [118]. A remarkable efficiency of 22.2% has been achieved, with typical module efficiencies of around 17–18% [119]. Research cell efficiency stands at over 25%, whereas the theoretical conversion efficiency limit for a silicon solar cell currently approaches 33% at 25˚C [120]. Therefore, given the theoretical performance limit of 29.4% with crystalline silicon-based solar cells, only slight performance enhancements are still feasible [119]. This limit is established by taking into account auger recombination and intrinsic losses, including but not limited to the thermalization losses of high-energy photons and the clarity of the absorber layer for subbandgap photons [121]. Perovskite and silicon-based solar cells can be successfully combined to create tandem solar devices that are promising to exceed the single-junction silicon devices currently dominating the photovoltaic market.

3.2. Recent Progress in Chemical Stability of Perovskite Solar Cells. Perovskite solar cells (PSCs) have recently improved their record efficiency from 9.7% to 20.1% [122]. However, there has not been much research done on the stability problems associated with these solar cells, which has limited their outdoor use. To obtain strong repeatability and extended durations for PSCs with high conversion efficiency, the problems of perovskite degradation as well as the stability of PSC devices need to be rapidly addressed. Exciting developments cannot be translated from the lab to industry and outside applications without studies on stability. Further investigation into the device's susceptibility to high temperatures has revealed that an increase from 300 to 375 K lowers PCE from 31.01% to 27.84% (for 4-T) and 18.56-16.14% (for 2-T) [5].

Atmospheric oxygen and moisture can directly impact the device stability of the components during assembly and testing. First, because $CH_3NH_3PbI_3$ is sensitive to moisture, the molecule tends to hydrolyze, which results in perovskite degradation. The following reactions occur during device degradation.

$$CH_3NH_3PbI_{3(s)} \longleftrightarrow PbI_{2(s)} + CH_3NH_3I_{3(aq)}, \quad (1a)$$

$$CH_3NH_3I_{(aq)} \longleftrightarrow CH_3NH_{2(aq)} + HI_{(aq)}, \quad (1b)$$

$$4HI\,(aq) + O_2\,(g) \longleftrightarrow 2I_{2(s)} + 2H_2O_{(1)}, \quad (1c)$$

$$2HI_{(aq)} \longleftrightarrow H_{2(g)} + I_{2(s)}. \quad (1d)$$

Accordingly, UV light, moisture, and oxygen are very important factors for the degradation of perovskite solar cells [123]. Furthermore, the equilibrium of reaction (1b) causes CH_3NH_3I, CH_3NH_2, and HI to coexist in the perovskite thin film. There are two main ways that HI can deteriorate in the next step [124]. One involves the redox reaction with oxygen present (1c). Another involves the photochemical process, which occurs when UV radiation causes HI to break down into H_2 and I_2 (1d) [125, 126]. The progression of the entire degradation process is fueled by the consumption of HI in accordance with reactions (1c) and (1d). Considering oxygen and moisture can both cause organic-inorganic halide perovskite to degrade, the majority of the fabrication process must be done in a glove box filled with inert gases such as helium or argon [127]. But when the constructed devices are measured in natural lighting, organic-inorganic halide perovskite generally experiences considerable deterioration. Perovskite deterioration would result in an unintended efficiency reduction, which limits the use of PSC outdoors [128]. Numerous studies have

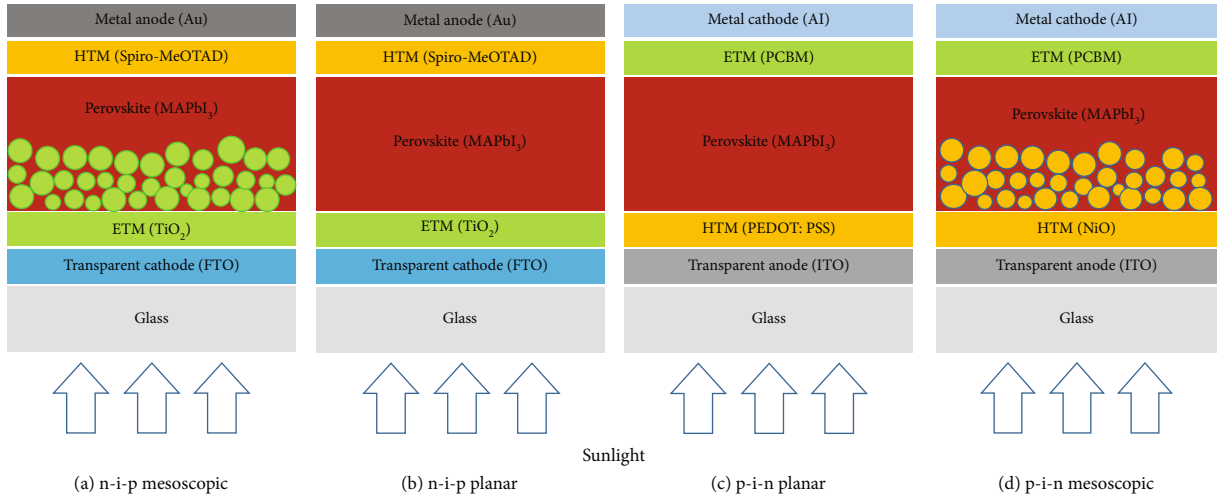

Figure 9: Classification of the mesoscopic and planar-shaped (n-i-p and p-i-n) perovskite devices [130].

explored how oxygen and moisture impact the overall stability of perovskite solar cells.

3.3. Perovskite Solar Cell Configuration. Perovskite solar cells offer a wider range of device structure than any other PV technology community. PSC devices are categorized according to their structure, morphology (mesoporous or meso-superstructure), and conductivity type (n- or p-type) (n-i-p or p-i-n and p-n or n-p devices) [129]. The perovskite structure is divided into two main categories: (i) normal/regular p-n types and (ii) planar, either n-i-p (conventional planar) or p-i-n (inverted planar), based on the electrical characteristics of the device whether electrons or holes have been collected at the bottom transparent conducting oxide (TCO). The two components of the traditional planar-designed perovskite device are (a) mesoporous and (b) meso-superstructure, as can be observed in Figure 9.

By using doped charge transport layers inside this device design, it was possible to fabricate p-i-n and n-i-p PSCs with a higher PCE of 20.3% [131, 132]. In both planar and mesoscopic heterojunction arrangement, HTM-free-based PSCs exhibit enhanced performance from 5.5% to 12.8% because of enhanced charge extraction [133]. Additionally, these developments were made possible by conducting interfacial engineering, optimizing the thickness of the transporting and perovskite layers, and introducing new scaffold layers [134]. The performance of PSC devices has not yet been fully explored with regard to variety of topologies, fabrication techniques, perovskite compositions, and charge-selective layers that have been proposed. The most effective absorbers contain lead, although various PSC architectures still have stability problems (ca. 13 mg m^{-2}). PSCs are also susceptible to elevated temperatures, UV radiation, moisture, and oxygen, which is a barrier to their commercialization [135].

3.4. Solar Device Performance Enhancement. The percent of solar energy which a PV cell can translate into usable power is referred to as power conversion efficiency. To compete against fossil fuel energy sources on price, solar module manufacturers have to increase efficiency rates [136]. The current theoretical maximum efficiency of solar modules is approximately 33% [137]. Plasmonic nanoparticles are one of the best approaches to increase efficiency of carbon-based perovskite cells [138, 139]. Also, metal nanoparticles diffract light when subjected to solar radiation, boosting its photocurrent within the cell and speeding up the production of free carriers [140]. It has been found that nanoparticles having scattering capabilities are equally effective than upconversion materials at increasing perovskite cells' efficiency by 1%. Changing the nanoparticle's size, shape, and distribution could result in even greater efficiency rates [141].

To boost the efficiency of PSCs, better light management can be used to reduce light loss from the cell. Utilizing transparent conducting oxide layers to reduce absorption losses and silicon oxide layers to harvest more sunlight is one approach to enhance solar cell efficiency [142, 143]. Surface gratings can improve internal reflection and increase internal reflection on a cell's surface thus increasing the cell's electrical and optical properties. The majority of solar cells can provide optimal efficiencies above 20% [140]. Accordingly, the efficiency of solar panels is influenced by cell efficiency, cell arrangement and design, and panel surface area [144].

The primary objective is to improve the device's performance while using an inorganic material such as $KSnBr_3$ as the photoactive layer. The device's performance is specifically compared to those of analogous devices that are theoretically and empirically designed. It was found that the device performed worse when the absorber contact had a larger fault density and the cell's optimal operating conditions were high at low temperatures. The following photovoltaic properties were obtained with the solar cell operating under ideal conditions: power conversion efficiency (PCE) of 19.5%, short circuit current density (J_{sc}) of 25.55 mA cm^{-2}, open-circuit voltage (V_{oc}) of 5.32 V, and fill factor (FF) of 14.68% [145]. Compared to similar solar cell technologies that have been computationally or practically studied, this PCE

Table 1: The effect of varying temperature on Voc, Jsc, FF, and PCE for a perovskite solar cell based on copper thiocyanide (CuSCN) hole transport layer [147].

Temp (K)	Voc (V)	J_{sc}	FF (%)	PCE (%)
260	1.9210	35.367021	39.69	26.96
270	1.5703	35.367897	47.72	26.51
280	1.3392	35.367246	54.97	26.04
290	1.1534	35.366813	62.58	25.53
300	1.0626	35.366642	66.53	25.00
310	0.9964	35.366514	69.41	24.46
320	0.9438	35.366119	71.61	23.90
330	0.9008	35.366236	73.23	23.33

value is larger. Although $KGeBr_3$ has appealing qualities, it is not frequently used because of high initial cost, intermittent energy source, use of a lot of space, small amount of pollution during manufacture, transport, and installation [145, 146]. The effects of changing a number of parameters on the general performance of the solar cell were carefully explored in this model. These variables include the operational temperature, back-contact metal work function, and the thickness of hole transport and electron transport layers. In addition to the hole transport and electron transport layers, doping densities and the density of the absorber layer's defects were considered. The simulation findings demonstrated that by adjusting the thickness of the absorber and its defect density as well as the width and doping densities of the hole transport and electron transport layers, the device's performance could be improved. It was found that the device performed worse when the absorber contact had a larger fault density. Nickel, platinum, and Pt metallic back contacts produced outcomes comparable to those of gold. As a result of their relative affordability, these metals can be used as substitutes for gold.

Similar to every other semiconductor device, solar cells are temperature-sensitive (Table 1). Temperature increases affect the majority of a semiconductor's material's properties since a semiconductor's band gap narrows [148, 149]. It is possible to interpret a semiconductor's band gap decreasing with temperature as an elevation of the material's electrons' energy. As a consequence, an increase in temperature results in a narrowing of the band gap [150]. The component primarily affected by an increase in temperature inside a solar cell is the open-circuit voltage.

4. Hole Transport and Electron Transport Materials

A critical component of perovskite solar cells is the hole transport material (HTM). Inverted (p-i-n) PSCs frequently use PSS, an organic HTM. Because of their inherent chemical stability and high cost, inorganic hole transport materials (HTMs) are the preferred options for selective contact materials. Inorganic HTMs with the appropriate characteristics such as the right energy level and high carrier mobility can enhance charge transport as well as increase PSC stability at ambient temperatures, and are cheap to fabricate [70]. While being unstable, costly, and acidic, PEDOT: PSS has the potential to harm the absorber [151]. Due to its qualities including low cost, simple synthesis, and high hole mobility, copper zinc tin sulphide (CZTS), an inorganic semiconductor, can be used as a HTM [152]. There are three major layers in a planar heterojunction perovskite-based solar cell which are sandwiched between the two conducting electrodes. Planar heterojunction perovskite-based solar cells typically have the architecture—hole transport material (HTM), back electrode, and electron transport material (ETM). Recent research has shown that improving the conductivity of hole transport materials through doping and increasing charge collection by altering the absorber thickness could have a positive influence on the efficiency of planar heterojunction-based solar cells [153]. Perovskite-based solar cells also require materials that can transport electrons, which is a critical component [154]. It is also possible to quantitatively simulate how alternative electron-carrying materials would affect the final performance of the PV device. Several PV factors, including absorber thickness and numerous PV characteristics such as the thicknesses of the absorber, HTM, and ETM, can be improved using simulation techniques and then put into practice by experimenters [153, 155]. The acceptor concentration and hole mobility of HTM, trap density, and back contact metal's work function have demonstrated a considerable impact on the device's performance [70]. Even with these significant advantages, it is still essential to improve the hole mobility as well as the conductivity of HTM, the stability of perovskite as well as the ETM, and the displacement of poisonous lead [156]. By appropriately synthesizing the perovskite absorbers, optimizing selective contact design, and increasing HTM and ETM conductivity, the device's performance and stability will be enhanced [153, 155]

From Table 2, highly efficient PSCs are obtained by using hole transporting materials (HTMs) which are necessary for removing and moving holes from the perovskite layer towards the electrodes. An effective HTM for a device with long-term stability is being developed using dopant-free HTMs in PSC devices with promising robust operational features [157]. Particularly, the various perovskite materials that distinguish HTMs based on their molecular or device architectures are used to classify perovskite solar cells. Figure 10 shows the various inorganic HTM materials usually applied in PSCs.

Table 2: Some of the HTMs utilized in perovskite solar cells [70, 133].

Review of organic, inorganic, and carbonaceous hole-transport materials for perovskite solar cell applications	(1) Inorganic HTMs: (i) *P*–type semiconductors-based HTMs: CuPc, CuSCN (ii) Transition metal-based HTMs (iii) Nickel & copper-based HTMs: NiO, CuI, Cu_2O, CuO, $CuCrO_2CuGaO_2$ (iv) MoO_3, V_2O_5, VOx, WOx (2) Organic HTMs: (i) Small molecule-based HTMs: pyrene, thiophene, porphyrin, carbazole (ii) Long polymer-based HTMs: Spiro-OMeTAD, fluorine doped Spiro- (iii) OMeTAD and MoOx (interlayer in Spiro-OMeTAD), PEDOT: PSS, P3HT, and PTAA (3) Carbonaceous HTMs/electrode: (i) Conducting carbon, CNTs, GO, r-GO

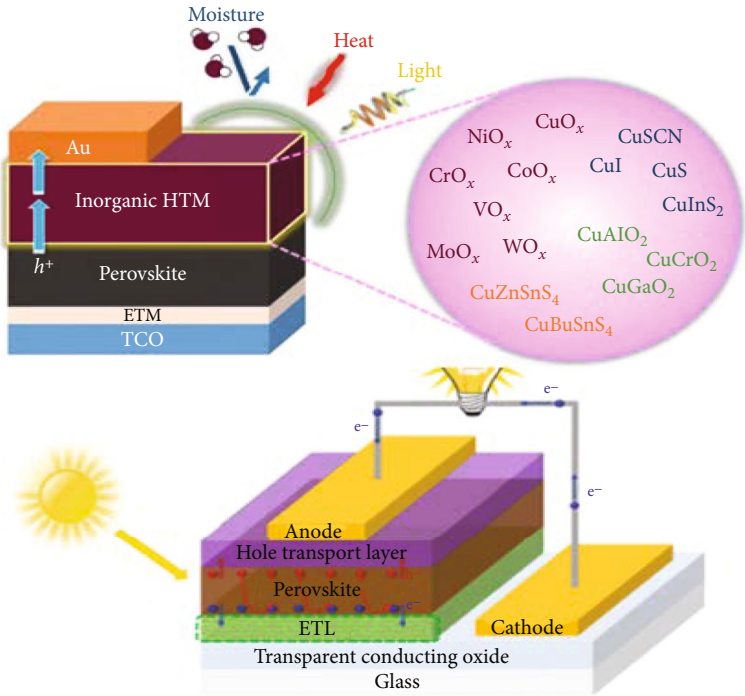

Figure 10: Inorganic HTM materials for a perovskite solar cell architecture [158].

The primary purpose of HTMs in solar cell device is to gather and transport excitons after the light harvester injects holes, effectively separating the electrons and holes, which is a significant and critical component of the PSCs [159]. An excellent HTM material has superior photochemical and thermal stability, long-term stability in air, acceptable energy levels that correspond with the perovskite layer, and intrinsically high hole mobility [160].

There are two types of HTMs for PSCs—organic and inorganic semiconductors. Inorganic HTMs such as CuSCN, CuS, $CuInS_2$, and CuI can have simpler, cheaper ingredients than organic HTMs, for instance, 1-(3-methoxycarbonyl)propyl-1-phenyl[6,6]C_{61}(PCBM) and Spiro-OMeTAD, although they often need to be deposited using more expensive non–solution-based methods such as sputtering, atomic layer, or pulsed laser deposition methods [161]. Since they do not need any dopants or additives and generally have greater intrinsic hole mobility than inorganic HTMs, they have better long-term stability. The main disadvantage, however, is that there are not as many options available as there are for inorganic HTMs. Most inorganic HTM devices have lower efficiency than organic-based HTMs [161]. Small molecules, polymers, and organometallic compounds are the three primary categories of organic semiconducting materials used for hole transport layers of PSCs [161].

The adjustment of the essential device design parameters is done to increase cell power efficiency. In perovskite solar cells, HTMs are used to collect and transport holes that have

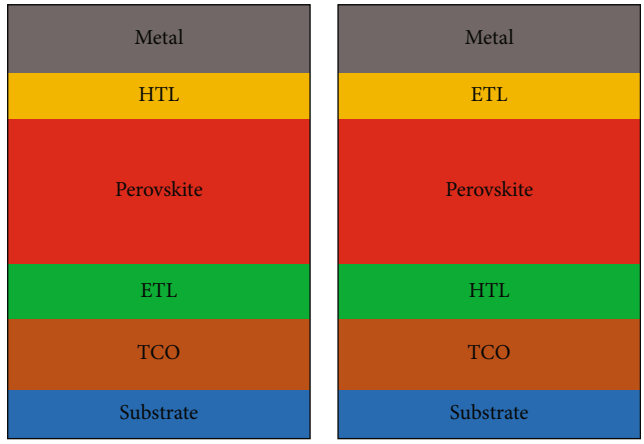

Figure 11: Perovskite solar cell structures (a) n-i-p and (b) p-i-n configurations [165].

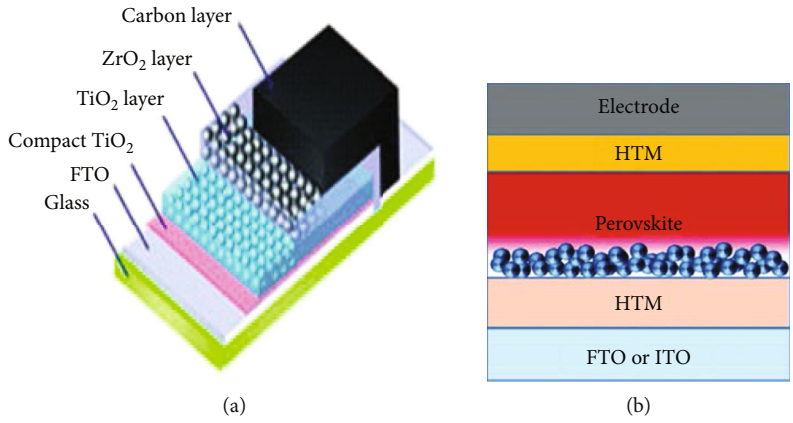

Figure 12: Mesoscopic perovskite solar cells [167].

formed within the perovskite absorber layer to the perovskite/HTM interface. Charge extraction through ETMs is very essential. For high-performance PSC devices, HTMs are necessary. Despite being efficient, these materials need a significant amount of doping with additives (for instance, nanoparticle, graphene, and ZnO, polyaniline) to increase charge mobility and substrate compatibility, which causes stability problems with HTMs as well as increased costs and experimental complexity [161]. Due to its excellent thermal stability, low cost, and appropriate energy level, TiO_2 has been widely employed as the best ETM for PSC [160]. Most recently, however, the use of zinc oxysulphide (ZnOS) has been proposed as a better electron transport material because of its stability against sulphurization, low toxicity, and robust tunable band gap [162]. A band gap is the distance between the valence band of electrons and the conduction band [163]. There are two main configurations of perovskite solar cells which include n-i-p and p-i-n configurations each of which is inverted relative to the other resulting in planar solar cells with minimal hysteresis and high efficiencies of 16.5% and 20%, respectively [164]. Examples of n-i-p and p-i-n solar cell architectures are presented in Figure 11.

To achieve excellent performance, planar perovskite solar cells with a p-i-n structure employ both hole-transport layers and electron-transport layers to enhance the collection of the photo-generated holes and electrons [166]. On the other hand, mesoscopic solar cell is third-generation solar technology. The ability to fabricate the absorber layer using a solution-based method is a noteworthy feature of mesoscopic solar cells. An example of a mesoscopic-based perovskite solar cell is presented in Figure 12.

4.1. Effects of Doping on ETM and HTM. Hole and electron transport materials are essential in the transport of excitons. Organic and inorganic p-type semiconductor materials have been frequently used for perovskite solar cell architectures [133]. The electrical conductivity of the layers within the solar cell design is determined by the doping of the photoactive material which will have an impact on the device's functionality. The overall performance of a device is enhanced by proper doping of HTM and ETM layers, which increases the interface electric field [168, 169]. There are two ways to dope HTM and ETM. The first is by using minority carriers that will significantly lower fill factor and efficiency and change the J-V curve's shape to an S [170]. Another relates to the

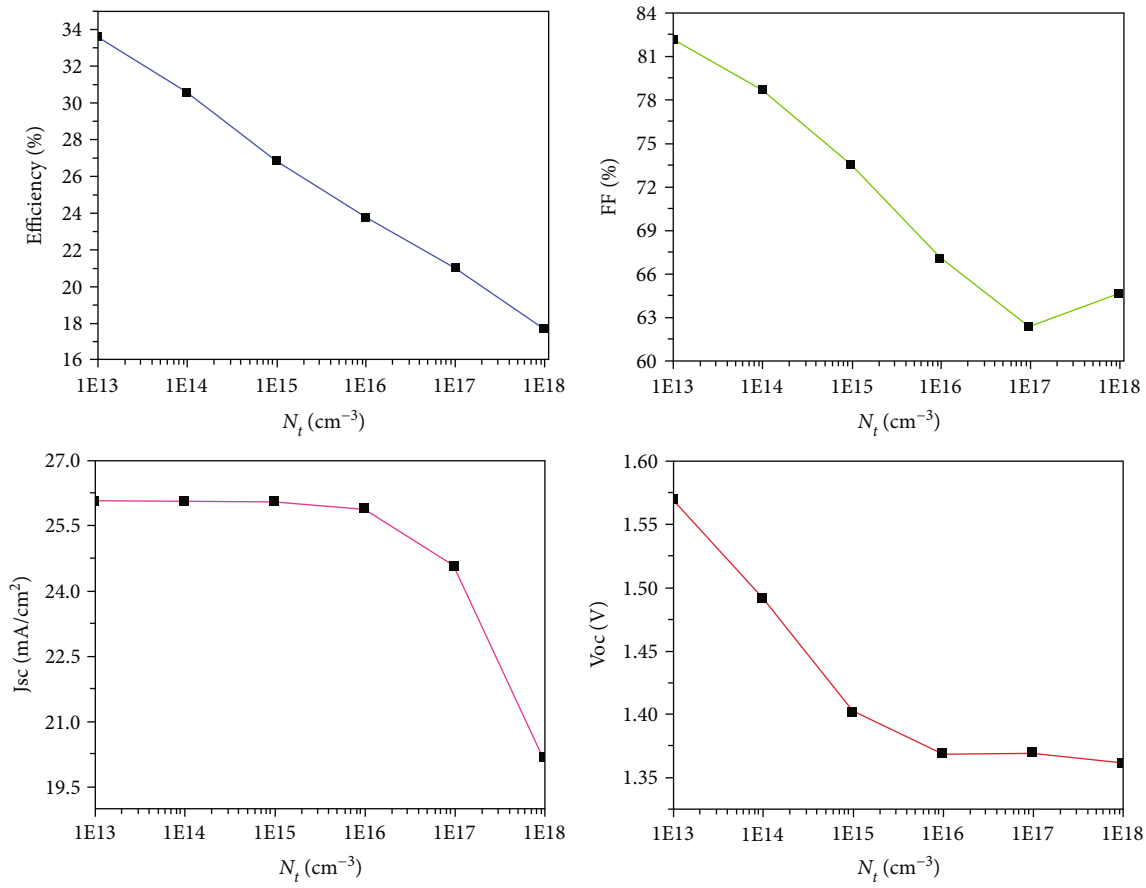

Figure 13: The influence of defect density on PV parameters [27].

majority of carriers which results in an increase in efficiency and fill factor. A better carrier transport and appropriate energy position can indeed be attained with mild doping doses [171]. Deep faults can be avoided by doping optimization and self-doping processes. To understand the doping effect of HTM and ETM on the device performance, the doping levels are varied from 10^{14} cm^{-3} to 10^{19} cm^{-3} [172]. Figure 13 represents the changes in the PV parameters with the defect density of HTM and ETM [27].

4.2. HTM and ETM Free Perovskite Solar Cells. HTM and ETM are necessary to obtain efficient photovoltaic performance; however, their effect in obtaining efficient solar cell performance is not equal [163]. This means that, upon the removal of HTM, there is direct contact between the photoactive layer and the glass such as indium tin oxide (ITO), which inhibits hole injection and consequently reduces cell performance. An excellent HTM should have high hole mobility, low electron affinity, compatible HOMO and LUMO energy levels with perovskite, high thermal stability and should involve low costs [65]. Technology computer-aided design (TCAD) Atlas has been used to design a number of ETM-free PSCs in order to improve device performance and lower fabrication costs [173]. According to simulations of PEDOT: PSS-$CH_3NH_3PbI_3$-PCBM as well as CuSCN-$CH_3NH_3PbI_3$-PCBM p-i-n PSCs has demonstrated a strong agreement with experimental results. In the ETM-free PSCs, various HTMs were chosen and mixed directly with n-$CH_3NH_3PbI_3$, with CuSCN-$CH_3NH_3PbI_3$ being the best HTM. The effects of the back electrode material, gradient band gap, thickness, doping concentration, and bulk defect density on the performance are examined in order to better understand the CuSCN-$CH_3NH_3PbI_3$-based PSC [174]. The design is optimized by using the energy band and the distribution of the electric field. The CuSCN-$CH_3NH_3PbI_3$-based PSC efficiency is thus increased [175]. HTL-free perovskite solar cells have attracted interest because of the numerous benefits including cost savings, a simpler manufacturing method, and the prevention of oxidation while enhancing stability and a longer lifetime [176]. Table 3 gives a preview of the performance of full perovskite, HTM-free, and ETM-free solar cell.

Table 3: The effect of cell architecture (PCM/perovskite/PEDOT:PSS/ITO) on the power conversion efficiency [177].

Cell architecture	PCE (%)
Full solar cell	~ 7.8
ETM free	~ 6.2
HTL free	~ 3.8

Currently, attention is shifting towards the minimalist device structure architecture of PSCs for rapid advances of

electron transport layer-free PSCs through composition and solvent engineering in order to achieve higher device performance and effective interface energy level alignment [163, 177]. In general, ETM and HTM are responsible for charge extraction, but when these materials are removed, the excitons cannot be extracted, efficiently resulting in hysteresis and poor cell performance [163, 177].

4.3. Hole Conductor Free Tin-Lead Halide Based All-Perovskite Heterojunction Solar Cells. In today's world, HTM-free PSCs with their straightforward construction and processing, low manufacturing cost, and excellent stability are very important [178]. An effective and novel HTM-free PSC structure with carbon serving as the back electrode, WS_2 serving as the ETM, and $CH_3NH_3Pb(I1xClx)_3/FA_{0.75}Cs_{0.25}Pb_{0.5}Sn_{0.5}I_3$ acting as a light the photoactive layer has been found to exhibit an optimal PV performance [179]. This structure was numerically investigated using the SCAPS-1D solar cell simulator. Also, a number of ETMs and solar cell layer characteristics, including absorber thickness, defect density, and doping concentration, were adjusted to find the best possible optimal values [180]. The device's best performance gave V_{oc} of 0.82 V, J_{sc} of 31.94 mA/cm^2, a fill factor of 77.95%, and PCE of 20.53% when carbon is used as the back contact [179]. When gold was used as the back contact, the cell parameters V_{oc} of 0.84 V, J_{sc} of 34.34 mA/cm^2, a fill factor of 78.54%, and PCE of 22.72% were attained [179]. A thin interfacial layer was inserted between the absorber and ETL to adjust the conduction band alignment also lead to increased PCE [181]. The architecture of the suggested structure comprised of Spiro-OMeTAD as the HTL, an absorber layer ($MAPbI_3$), and an ETL layer, CdS [182]. The doping densities of the ETL and HTL as well as the thickness of the perovskite solar layers were adjusted in order to achieve the highest PSC performance prior to the insertion of the interfacial layer. The highest power conversion efficiency of 18% [181] at a thickness of 250 nm for ETL, 400 nm for absorber, and 200 nm for HTL, respectively, with doping densities of 10^{22} cm^3 for ETL and 10^{19} cm^3 for HTL [181].

Due to its application as a light harvester in photovoltaic cells, the inorganic-organic perovskite is currently receiving a lot of interest. Tin–lead halide perovskites have a considerable chance of being used as energy harvesters in mesoscopic solar cells with heterojunction due to their high optical absorption, high carrier mobility, and good stability. The tin–lead halide perovskite's ability to serve as both a light harvester and a hole conductor in the photovoltaic panel is one of its special qualities in device application [183]. The p-type behavior as well as band gap of the various perovskites are revealed by surface photovoltage as well as optoelectronic properties [184]. In order to achieve both low toxicity and excellent performance of perovskite solar cells, the combination of tin- (Sn-) lead iodide perovskite is thought to be the most attractive low-bandgap photovoltaic material (PSCs) [185]. Their performance, however, still falls short of that of the complete Pb-based equivalent. One of the key elements that significantly influences how well a PSC performs is the HTL [186]. For instance, the band gap and also the resilience of the layers may be affected by changes in the ratio of the methylammonium (MA) to formamidinium (FA) cations during the annealing procedure. The pure $MAPbI_3$ as well as the $FAPbI_3$ solar cells are more stable than their mixture when it comes to the PV characteristics at various temperatures [187].

Here, the $(FASnI_3)_{0.6}(MAPbI_3)_{0.4}$ PSCs with such an inverted structure have been successfully created using a CuI/PEDOT:PSS bilayer structure as the HTL [185]. The CuI/PEDOT:PSS film is seen to have a smooth shape and good interfacial contact, and the CuI injected can partially impact the crystallization behavior of $(FASnI_3)_{0.6}(MAPbI_3)_{0.4}$and can promote the growth of high-quality perovskite films [188]. In addition, the high mobility of CuI and the cascading energy alignments in the device enables effective hole extraction as well as transport from the perovskite to the anode [188]. Moreover, the electrochemical impedance spectroscopy measurement showed that the photovoltaic performance is observed to be highly influenced by the concentration of CuI, which controls its thickness. Therefore, by employing a double-layer CuI/PEDOT:PSS as HTL with a CuI concentration of 10 mg/mL, the produced PSCs based on 60% Sn perovskite results in an increased high power conversion efficiency of 15.75% with negligible J-V hysteresis [185]. The PSCs exhibit enhanced stability, which is an essential quality for the development of high efficient PSCs which is attributed to the double HTL of CuI/PEDOT:PSS [185].

4.4. Effect of HTMs on the Efficiency PSCs. Hole transport materials are essential for extracting holes from a perovskite layer by conveying the holes to the counter electrode, and preventing the flow of electrons back to the metal electrode [189]. Furthermore, HTMs placed on the perovskite layer could shield the delicate layer from disintegration brought on by exposure to ambient air [128]. Accordingly, improving the effectiveness and lifetime of PSCs requires careful consideration in HTM design. Although many organic HTMs have been fabricated with satisfactory efficiency, it is still unclear how molecule shape affects how well HTMs work. Isomers, which are available to study the structure-property relationship of HTMs, have distinct electronic properties but the same chemical content as well as highly similar molecular structures [190]. The effects of the heteroatom and the addition of double bonds to the conjugation on the molecular optical, electrochemical, hydrophobic, film-forming, and photovoltaic performance in PSCs have been explored. Higher hole mobility and enhanced hole extraction ability are produced by the molecules with double bonds due to their significantly improved planarity and intermolecular charge transfer [191].

4.5. The Metal Back Contact in PSCs. Metal back contacts in photovoltaic cells should result in the design of low-cost, chemically resistant, and easily processed and fabricated photovoltaic cells. The back contact of a PV cell is essential in ensuring effective charge transport to the cell's external circuit. Since the onset of PV cells, gold has been the default back contact for PSCs, with the function of carrying charges from the HTM to the external circuit. However, the high cost of Au has hindered the fabrication of PSCs in large

Table 4: Effects of altering metal back contact on J_{sc}, FF, and PCE [162, 192].

Back contact type	Metal work function (eV)	Voc (V)	J_{sc}	FF (%)	PCE (%)
Silver	4.26	0.9115	35.246924	35.15	11.29
Tin	4.28	0.8604	35.256642	39.28	11.92
Titanium	4.33	0.8272	35.278009	46.23	13.49
Vanadium	4.50	0.8258	35.330082	65.08	18.99
Iron	4.50	0.8258	35.330082	65.08	18.99
Tungsten	4.55	0.8433	35.341368	69.21	20.63
Molybdenum	4.60	0.8898	35.351059	70.73	22.25
Copper	4.65	0.9625	35.358882	69.69	23.72
Cobalt	5.00	1.0626	35.365407	66.53	25.00
Gold	5.10	1.0626	35.365407	66.53	25.00
Palladium	5.12	1.0626	35.365407	66.53	25.00
Nickel	5.15	1.0626	35.365407	66.53	25.00
Platinum	5.65	1.0626	35.365407	66.53	25.00

scale. For this reason, it is critical to investigate different metal back contacts that can be used in place of Au. Platinum is a noble metal that is frequently employed in dye-sensitized solar cells (DSSC) and could as well be used in perovskite solar cells. Although platinum is significantly less expensive than gold, the problems associated with cost and abundance remain; hence it has not been given much consideration in the PSC devices. The key criteria for selecting alternative metals are strongly tied to ensuring a high PCE and strong stability under external aging circumstances, beside the cost-related considerations. Table 4 discusses some of the efforts made to replace gold with alternative metal back contacts.

It is observed from Table 4 that the metal work function values increase from 4.26 to 5.1 eV while power conversion efficiency increases from 11.29 to 25%. A work function of 5.1 eV [193] for gold gives an optimum cell operation. Nonetheless, other metals can also be used in place of gold which is not only expensive but can also migrate across the HTL into perovskite films, resulting in the degradation of the devices [194]. Therefore, alternative metal back contacts such as Pd and Ni that are cheap and readily available, with similar operational performance as gold have been tested. Moreover, nickel, platinum, and Pd metallic back contacts also produced results comparable to those of gold. Due to their relative affordability, several metals can be utilized as gold substitutes. Also, due to the synergistic effect of perovskite decomposition and metal migration, both Au and Ag can react with the halide ions in the hybrid perovskite solar cell [195]. But since the perovskite layer is directly lit when the devices are working, the back contact architecture employed in p-i-n design can reduce transmission losses.

Perovskite solar cells have shown to be particularly useful due to their widespread availability, low cost, and improved efficiency. PSCs are the fourth-generation solar cells with back contacts and a light-absorber layer made of either a hybrid organometallic halide or an inorganic perovskite material. The other components are the electron transport layer and the hole transport layer which enable charge extraction. This implies that there are different forms of perovskite which include organic-inorganic hybrid perovskite, lead-based perovskite and all-inorganic perovskite solar cells. As a result, perovskite solar cells have gained popularity and are believed to revolutionize the photovoltaic industry. For photovoltaic technology to be commercially viable, it typically needs to have at least a 20-year operating lifespan with less than a 10% efficiency decline in performance [196]. Compositional engineering, interface engineering, as well as the development of all-inorganic perovskite and encapsulation techniques, have all been heavily focused on in order to improve the intrinsic stability and extrinsic stability, and as a result, significant success has been achieved [33].

5. Solar Cell Fabrication Approaches

There are various methods which are employed in solar cell fabrication. The major methods are herein discussed. The fabrication methods which comprise vacuum and non-vacuum techniques, are touted to significantly improve the efficiencies of PSCs because PSCs, dye-sensitized solar cells (DSSCs), and thin-film PVs share similar structural architectures [197]. However, the actual study has revealed something different [198], despite having a reasonably simple process and high output efficiency. Several alternative non–vacuum-based strategies have been proposed. Some of the processes like screen printing and doctor blading have been effectively used for the production of large-scale perovskite films [199]. The only vacuum-based technique that has ever been proven to produce good cell performance is thermal evaporation. The sputtering approach has rarely been used, either because there is no good target for it or because high-energy species might harm perovskite materials resulting to poor stability. The fabrication methods of PSCs can be divided into various categories which include one-step process, two-step process, vapor-assisted process, and thermal evaporation processes among others [200].

The term "solar manufacturing" refers to the production and assembly of components for the entire solar value chain with solar photovoltaic (PV) panels being the most

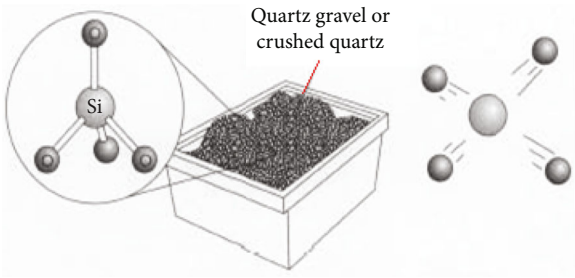

Figure 14: Silicon-based solar cell prepared using quartzite gravel [203, 204].

dominant examples. PV panels are made up of numerous subcomponents, including wafers, cells, glass, back sheets, and frames [201, 202]. With silicon accounting for over 95% of the modules supplied today, silicon is by far the most prevalent semiconductor material for use in solar cell technology. An example of a silicon-based solar cell preparation method is illustrated in Figure 14.

Pure silicon, a substance that is not pure in its natural state, is the primary component of silicon-based solar cells. In order to create solar cells, silicon dioxide from either crushed quartz or quartzite pebbles is first added to the electric arc furnace, in which a carbon arc is used to liberate the oxygen. Molten silicon and carbon dioxide are the end products, as can be noted in equation (2).

$$SiO_2(g) + 2C(s) \longrightarrow 2CO(g) + Si(s) \quad (2)$$

At this point, silicon still needs to be purified before it can be utilized for solar cell manufacture [205, 206]. The key to the only vacuum-based technique that has ever been proven to produce good cell performance is thermal evaporation, although other techniques can not be ruled out. To the best of our knowledge, sputtering has never been used, either because there is not a good target for it or because high-energy species might harm these unstable perovskite materials. The fabrication methods of PSCs can be divided into four categories: one-step process, two-step process, vapor-assisted process, and thermal evaporation process, which is to liquefy it, clean it with distillation, and then deposit it into a silicon seed sample, among other methods such as spin coating, and thermal evaporation. High towers are where chemical cleaning is typically used before proceeding into the reaction chamber. Here, ultrapure silicon is created from filtered gas [207]. Boron is added to silicon during the manufacturing process to allow for the flow of electrons, and phosphorous is then diffused into silicon during the processing of cells. In order to create a semiconductor that can conduct electricity, the resulting pure silicon is doped using phosphorous or boron to create an excess of electrons that can reach the conduction band [208]. The bright silicon disks need an anti-reflective coating, often made of titanium dioxide.

Typically, two layers are formed, and the space between them acts as a wall for the electrons, preventing them from getting beyond the barrier on their own but allowing them to do so with the aid of photons [209]. More electrons usually collect on the cell's upper side, where they push one another aside. Electrons may rotate through wires that are connected to the top of the cell [210]. Boron is used for doping, which introduces impurities, and crystallization, which melts the mixture. Unwanted contaminants are removed through regulated cooling. After the silicon brix has hardened, it is withdrawn and then sliced into films that are <0.2 mm thick. These slices are then utilized to make solar cells [211]. Wafering is done in two steps: first, the brix is cut into slices, then the slices are pushed into the wire sole, and finally, the long wire holding the slurry is inserted through the brix. It has a number of silicon carbide, which removes the wafer from the brix, after which they are cleansed and brought to the neighboring cell plate [212].

5.1. Spin Coating. Spin coating is a useful technique for applying homogeneous thin layers of exceptionally sticky or hydrophobic polymers to planar oraxi-symmetrical substrates. Utilizing centrifugal force, spin coating uses a liquid-vapor interface to deposit a homogeneous film on a solid surface. A liquid is typically placed in the middle of a circular surface and quickly spun to create uniform sheets that range in thickness from 1 to 10 microns [213]. In this method, a tiny drop of coating material is put into the substrate's center before the substrate is rotated at a regulated high speeds. The substrate spins during spin coating process around an axis that must be parallel to the area to be coated [214]. As a result, a thin coating film forms on the surface as the coating material extends toward and eventually moves away from the substrate's edge. The type of coating (viscosity, drying rate, % particles, surface tension, etc.) and the spin process parameters, such as rotation speed, determine the final film thickness and other attributes of the device [215]. The spin coating technique for the preparation of solar cell device is presented in Figure 15. Two-dimensional lead halide perovskites (2D perovskite) have emerged as ambient stable photovoltaic materials owing to their unique layered structure.

5.2. Thermal Evaporation. A well-established technique for coating a thin layer is thermal evaporation, whereby the material evaporates in a vacuum as a result of high-temperature heating, thus allowing the vapor particles to move and immediately contact a substrate where they again transform into a solid material [217, 218]. However, it is challenging to precisely regulate the thickness and create a uniform surface when using the spin-coating method to deposit perovskite films. To address these bottlenecks, the thermal evaporation method was recommended. Compared to the spin-coating approach, this technique offers superior reproducibility and film quality [219]. Thermal evaporation phenomenon illustration is presented in Figure 16.

5.3. Inkjet Printing. One of the most efficient methods for producing large perovskite solar cells is inkjet printing. However, the produced perovskite film appears discontinuous with escalating flaws because ink crystallizes immediately after printing. It significantly limits the use of inkjet printing technology for producing perovskite photovoltaic systems [222]. Using printed perovskite solar cells,

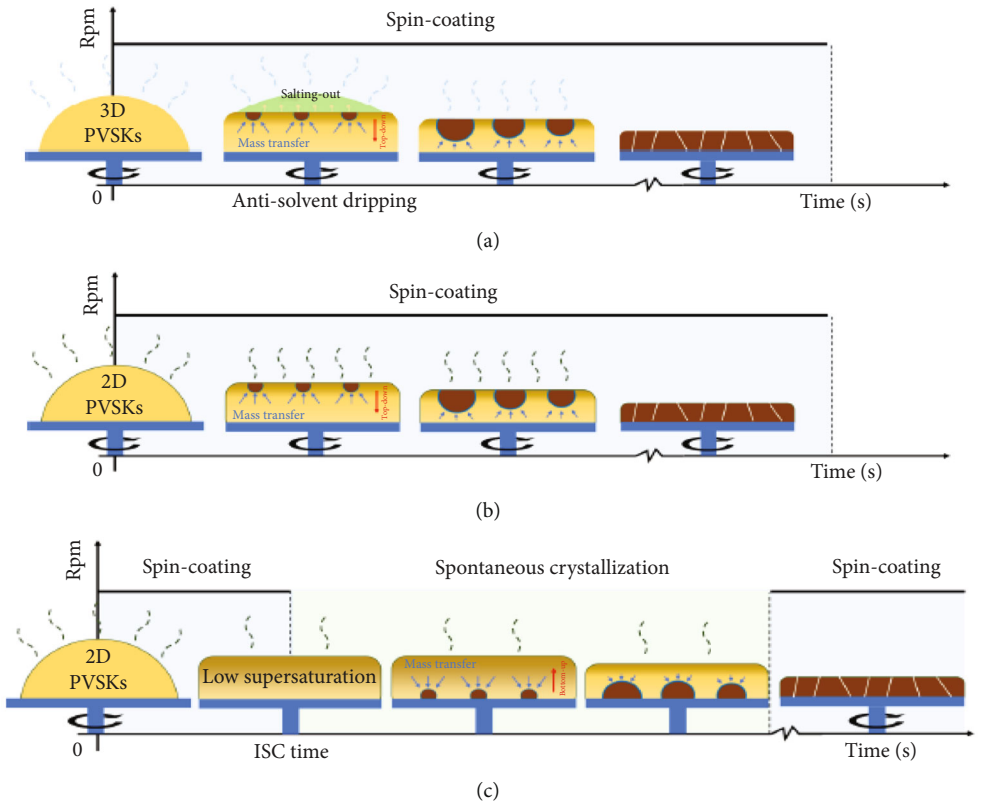

FIGURE 15: Spin coating preparation for a self-supporting ultrathin film. Conventional downward crystallization by an antisolvent dripping in 3D perovskite (a) and direct spin-coating in 2D perovskite (b) and upward crystallization by the intermittent spin-coating method in 2D perovskite (c) [216].

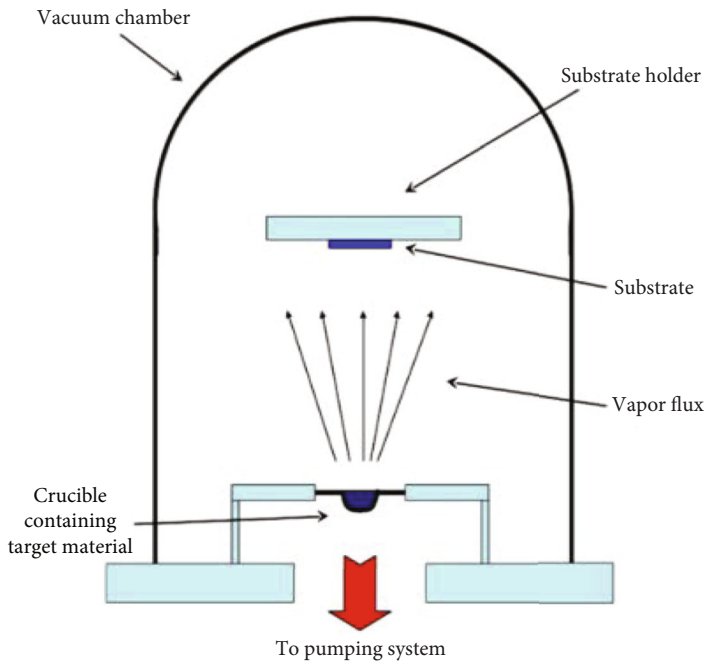

FIGURE 16: The thermal evaporation approach in the preparation of PSCs [220, 221].

noncontact inkjet printing allows quick and digital deposition together with robust control over layer formation J-V properties of the 0.04 cm^2 [223].

Since it provides new opportunities in a range of applications, such as tandem cell design and building-integrated photovoltaics, semi-transparency is a desirable and significant characteristic in solar cells. Metal halide perovskite can be produced as a thin film and possesses the ideal characteristics to serve as a photoactive layer in solar cells, although its chemical makeup can alter its band gap [224]. The solar cell's efficiency is typically compromised when great transparency is achieved. Semi-transparent perovskite solar cells can be created via ink-jet printing without relying on their composition or thickness [225]. The method is based on a technology that may be scaled up. Inkjet printing of arrays of transparent pillars that are made of inactive photopolymerizable liquid compositions and partially covered by the perovskite are possible to design. The transparency and efficiency of the solar cells can be digitally controlled by printing this material at specified locations and array densities [226]. Without an upper metal contact, this new semitransparent architecture exhibits 11.2% efficiency and 24% average transparency [226]. The $J - V$ curves generated from inkjet-printed photovoltaic device of the configuration OMeTAD/$Cs_{0.05}MA_{0.14}FA_{0.81}PbI_{2.55}Br_{0.45}/C_{60}/TiO_2$/FTO in various solvents is presented in Figure 17.

It is evident from Figure 17 that solvent effects play a critical role in the cell performance. For instance, printing the cell device architecture in a binary mixture of N-Methyl-2-Pyrrolidone (NMP) and dimethyl formamide (DMF) gave a cell with good operational I-V characteristics compared to one printed in a binary mixture of dimethyl sulfoxide (DMSO) and dimethyl formamide or in dimethyl formamide (DMF).

5.4. One-Step Method. Due to its simpler operation and lower cost, the one-step deposition approach has frequently been used in the manufacture of perovskite solar cells. With careful management of the perovskite precursors, the perovskite film may be produced with an appropriate stoichiometry and without any pinholes [227]. Typically, gamma-butyrolactone (GBL), dimethylformamide (DMF), dimethyl sulfoxide (DMSO), or a combination of two or all three solvents has been used to dissolve organic halides methylammonium/formamidinium iodide (MAI/FAI) and inorganic halides such as PbI_2. To create a dense, phase-pure, and pinhole-free perovskite layers, the precursors are mixed and subsequently spin-coated and annealed at temperatures between 100 and 150°C [228]. As-produced MAI in commercially available $PbCl_2$ were dissolved in DMF in a 3:1 molar ratio in order to alter the halide anion ratio [229] which establishes a remarkable starting point for the one-step method with a 10.9% power conversion efficiency. After 30 s of spin coating and 100°C of postannealing, the perovskite layer is formed [230].

5.5. Two–Step method. The two-step perovskite deposition process does not require complete precursor preparation; instead, PbX_2 (X=Cl, Br, or I) and MAI/FAI layers must be separately spin coated [231, 232]. On a substrate, a PbX_2 seed layer is first created by spin-coating or doctor-blading. The inclusion of the MAI/FAI would then be completed by either spin-coating with the MAI/FAI solution or dipping the PbX_2-coated substrate into the solution, often isopropanol. After proper baking, the finished perovskite films would have been created [231, 233]. The appearance and quality of perovskite films may be better controlled by changing parameters in either phase thus making it more process-tunable than the one-step technique, despite the steps becoming more complex [234]. Figure 18 represents an example of a two-step DMSO-aided procedure.

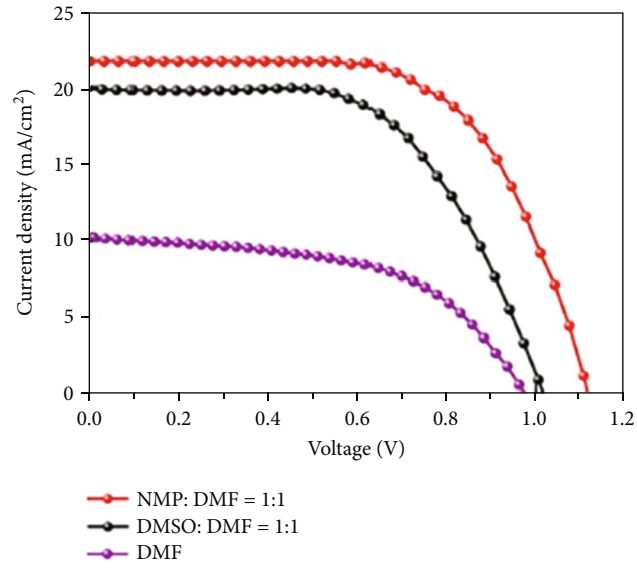

Figure 17: The current-voltage properties of a 0.04 cm^2 inkjet-printed photovoltaic cell of the configuration–OMeTAD/$Cs_{0.05}MA_{0.14}FA_{0.81}PbI_{2.55}Br_{0.45}/C_{60}/TiO_2$/FTO in NMP:DMF, DMSO:DMF, and DMF solvents [223].

5.6. Pulsed Laser Deposition. A high-intensity pulsed laser beam is used in the thin film deposition process known as pulsed laser deposition (PLD) to vaporize a target material before depositing it as a thin film on a substrate. It is a method for creating thin films where physical vapor deposition using PLD approach is applied [236]. The pulsed laser deposition approach has benefits over other methods, including stoichiometry, adaptability, versatility, reduced deposition temperature, and ability to develop metastable substances. Pulsed laser deposition is utilized more often in materials research because of these benefits [237]. For the purposes of solid oxide fuel cells, light-emitting diodes, and solar cells, thin films have been produced using the pulsed laser deposition technique [220].

The layer of material to be deposited is focused by a pulsed laser beam with a pulse duration of 10 to 50 ns [238]. Each laser pulse causes a little amount of the substance to be vaporized with the appropriate energy fluency (1–5 J/cm^2). The substrate is generally placed opposite the target where it receives a plume of the ablated material that is expelled from the target during ablation. Figure 19(a)

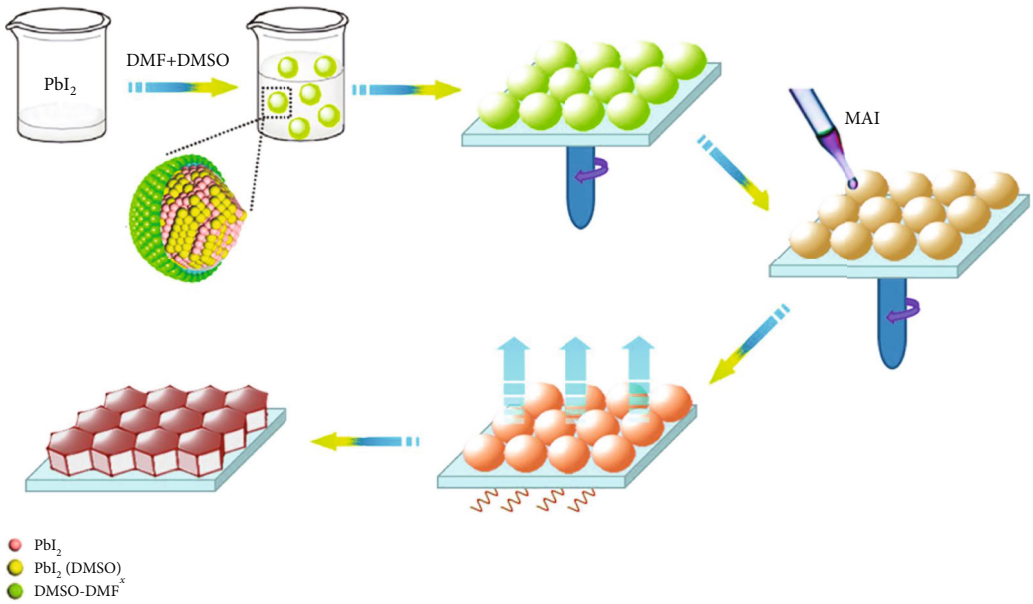

Figure 18: A two-step DMSO-aided synthesis of $MAPbI_3$ perovskite film [235].

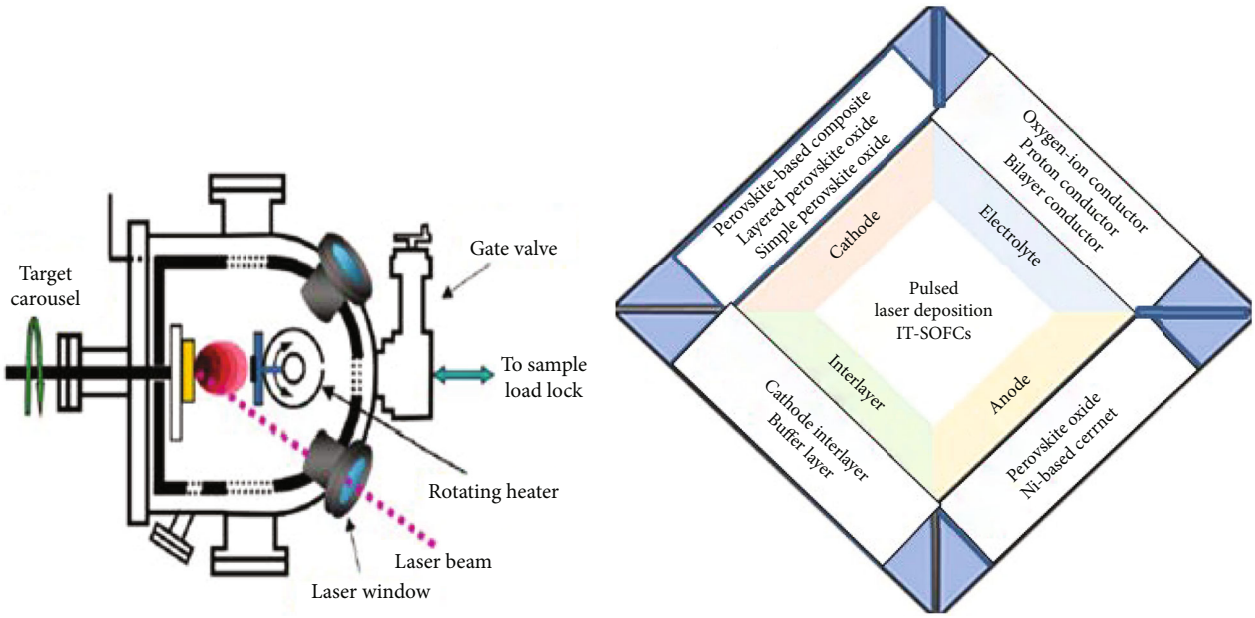

Figure 19: Pulsed laser deposition system's schematic diagram (a) and fabrication of thin films using PLD technique (b) [236, 239].

illustrates a pulsed-laser deposition system, whereas Figure 19(b) presents the cell architecture from the PLD technique.

5.7. Quantum Dots. Due to its remarkable optoelectronic features and straight-forward fabrication methods, lead halide perovskite quantum dots (PQDs), sometimes known as perovskite nanocrystals, are regarded as one of the most promising groups of photovoltaic materials for solar cells [240]. Because of their distinctive optical characteristics such as variable wavelength, restricted emission, and high photoluminescence quantum yield (PLQY), perovskite quantum dots (PQDs) have recently attracted a lot of attention [241]. The stability of PQDs needs to be further enhanced for industrial applications such as lighting and backlight devices in order to stop their degradation due to heat, oxygen, moisture, and light. Unstable PQDs could easily be degraded by oxygen and moisture [242]. Crystal formation from simple ion migration may reduce the PLQY of PQDs. Important techniques for addressing such issues include surface coating and better band alignment [241].

Compared to their bulk and quantum well equivalents, semiconductor quantum dots (QDs) have already been acknowledged as advantageous optical gain materials. Due to

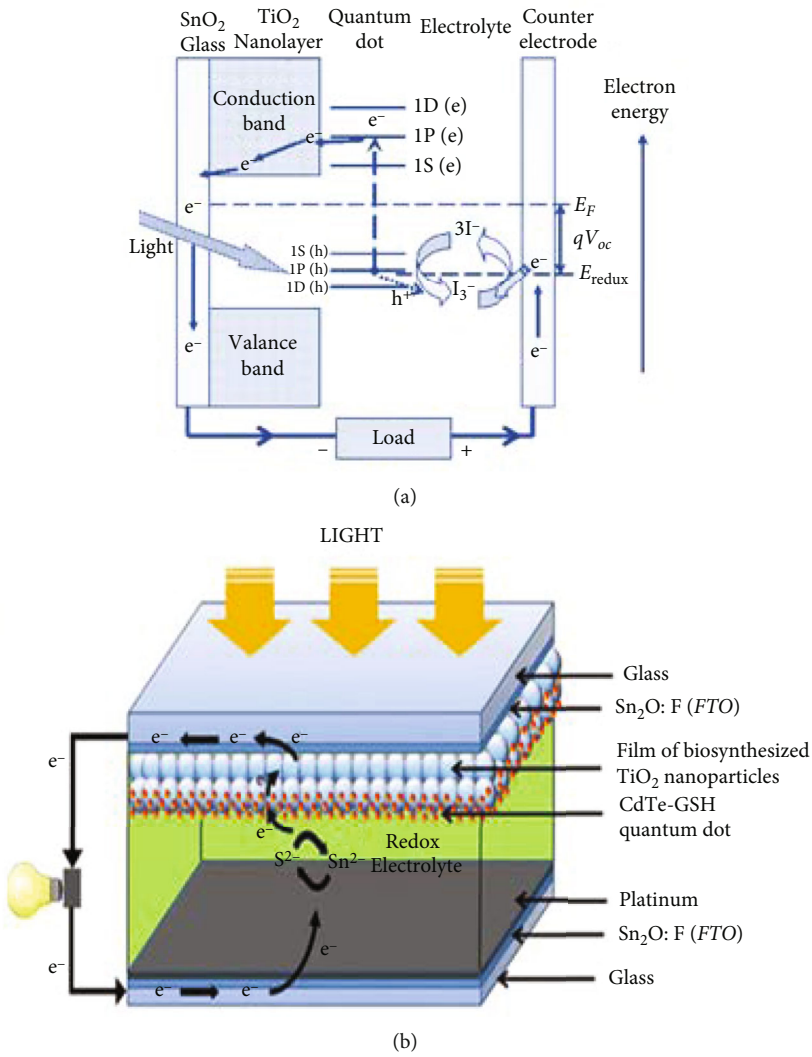

Figure 20: Quantum dot-sensitized photovoltaic cell structure and operation (a) and fabricated cell architecture (b) [243].

the 3D quantum confinement effect, QDs have well-separated delta function-like densities of states, size-tunable emission wavelengths, and strong optical oscillators, which promise low-threshold but also temperature-insensitive optical gains [242]. An illustration of quantum dot preparation device is presented in Figure 20(a), while the cell architecture prepared using this approach is shown in Figure 20(b).

6. Numerical Simulation Strategies

Various simulation softwares such as Personal computer one-dimensional (PC 1D), Accelerated mobile pages (AMPs), COMSOL Multiphysics, Technology computer-aided design (TCAD), the general-purpose photovoltaic device model (GPVDM), and Silvaco ATLAS, have been used to optimize the electrical properties of solar cell designs [244]. This review will, herein, consider a few numerical simulators commonly applied in solar cell analysis.

6.1. Solar Cell Capacitance Simulator. The 1-dimensional solar cell capacitance simulator (SCAPS-1D) was developed under the direction of Prof. Burgelman of Ghent University, Belgium [245–247]. The simulation model clarifies the foundation of solar cells and reveals the key variables that affect how well solar cells perform. The three fundamental equations for semiconductors—the Poisson, the continuity, and the equations for holes and electrons—are numerically solved in the simulation application. The Poisson and the continuity equations serve as the foundation for the SCAPS-1D program [248]. Because of its benefits, including ease of use and control, SCAPS-1D has been used in numerical simulation of solar cells. Equation (3) gives the Poisson expression.

$$\nabla^2\psi = \frac{q}{\varepsilon}(n - p + N_A - N_D). \tag{3}$$

Here, ψ is the electrostatic potential, N_A is the acceptor concentration, and N_D is the donor concentration. The explanations for the continuity equations are expressed according to equations (4) and (5)

$$\nabla . J_n - q\frac{\partial n}{\partial t} = +qR, \tag{4}$$

where R is the rate of carrier recombination and J_n is the current density of electrons.

$$\nabla . J_P + q\frac{\partial p}{\partial t} = -qR. \tag{5}$$

Here, J_P is the current density for holes.

Furthermore, equations (6) and (7) define the drift-diffusion current relations.

$$J_n = q_n U_n E + qD_n V_n, \tag{6}$$

where D_n represents the electron's diffusion coefficient.

$$J_P = qpU_p E - q\Delta_p. \tag{7}$$

Here, D_p is the hole diffusion coefficient.

The continuity equations are given by

$$\begin{aligned} \frac{dn}{dt} &= \frac{1}{q}\frac{dJn}{dx} - (U - G), \\ \frac{dp}{dt} &= -\frac{1}{q}\frac{dJp}{dx} - (U - G), \end{aligned} \tag{8}$$

where the recombination and generation rates are U and G.

Transients or switching times are unnecessary since solar cells function is in a constant state. The carrier concentrations for thermal equilibrium, other than steady state-conditions do not change over time. This can be shown by equations (9), (10), and (11).

$$\frac{dn}{dx} = \frac{dp}{dt} = 0. \tag{9}$$

This reorganizes the equation above such that

$$\frac{1}{q}\frac{dJn}{dx} = U - G, \tag{10}$$

$$\frac{1}{Q}\frac{dJp}{dx} = -(U - G). \tag{11}$$

SCAPS-1D simulation gives important photovoltaic characteristics such as the Fill factor (FF), short-circuit current (J_{sc}), open circuit voltage (V_{oc}), and power conversion efficiency (PCE) [249]. Furthermore, the program calculates the recombination profiles and energy band diagrams. The equations for calculating FF and V_{oc} are herein presented as (12), (13), (14), and (15).

$$\mathrm{FF} = \frac{\mathrm{V_{MP}I_{MP}}}{\mathrm{V_{OC}I_{SC}}}. \tag{12}$$

Empirical Fill factor

$$\mathrm{FF} = \frac{\mathrm{V_{OC}} - \mathrm{In}(\mathrm{v_{oc}} + 0.72)}{\mathrm{V_{OC}} + 1}. \tag{13}$$

and the $\mathrm{V_{OC}}$ is determined from equations (13) and (14).

$$\mathrm{V_{OC}} = \frac{\mathrm{kT}}{\mathrm{q}}\mathrm{In}\left[\frac{(\mathrm{N_A} + \Delta \mathrm{n})\Delta \mathrm{n}}{\mathrm{n_i^2}}\right], \tag{14}$$

$$\mathrm{V_{OC}} = \frac{\mathrm{nKT}}{\mathrm{q}}\mathrm{In}\left(\frac{\mathrm{I_L}}{\mathrm{I_O}} + 1\right). \tag{15}$$

The equation for the short-circuit current density can be approximated by the expressions (16) and (17), respectively

$$\mathrm{J_{SC}} = \mathrm{qG}(\mathrm{L_n} + \mathrm{L_P}), \tag{16}$$

$$\mathrm{I_{SC}} = \mathrm{J_{SC}A}. \tag{17}$$

In this case, G stands for generation rate, L_P and L_n stand for hole and electron diffusion lengths, whereas A represents the area of the cellin cm^2, I_L is light generated current, I_0 saturation current, kT/q is the thermal voltage, N_A is the doping concentration, Δ_n is the excess carrier concentration and n_i is the intrinsic carrier concentration.

The one-dimensional equations that affect the conduction of the charge carriers in semiconductor materials when they are in a stable condition are numerically solved using SCAPS-1D software. The one-dimensional SCAPS-1D program is used to carry out numerical simulations of p-p-n perovskite solar cells. The single-shot calculation of the SCAPS-1D simulation software is based on solving the Gummel iteration scheme with Newton-Raphson sub-steps wherein the initial step of the calculation starts with a simple guess of assuming null value for the quasi-Fermi levels throughout the solar cell architecture [250]. An illustration of the SCAPS panel for setting simulation devices is presented in Figure 21.

6.2. Silvaco ATLAS. The two- and three-dimensional device simulator ATLAS is based on physical principles. It makes predictions about the electrical characteristics of specific semiconductor architectures and offers information about the internal physical processes involved in the functioning of the device [251]. Moreover, Silvaco provides an extensive tool set for the development, enhancement, and analysis for digital cell libraries, allowing Integrated (IC) design teams to investigate the effects of various device models, design principles, and cell topologies in order to enhance the efficiency of their state of charge sparse optimal control (SoCs).

A technology computer-aided design (TCAD) simulation may not only show you how well the reverse current-voltage graph appears, but it can also explain why the device is failing. TCAD can be used to express device and process modifications effectively, saving manufacturing cycle times while highlighting possible performance enhancements. Test theories in TCAD is excecuted by manipulating model parameters and coefficients to alter how different physics

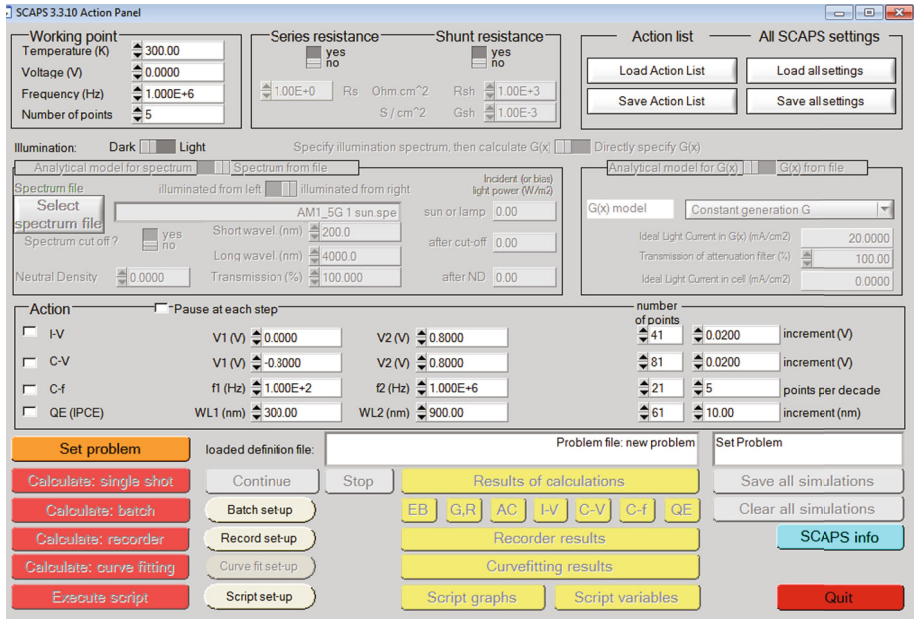

Figure 21: SCAPS-1D graphical user interface [153].

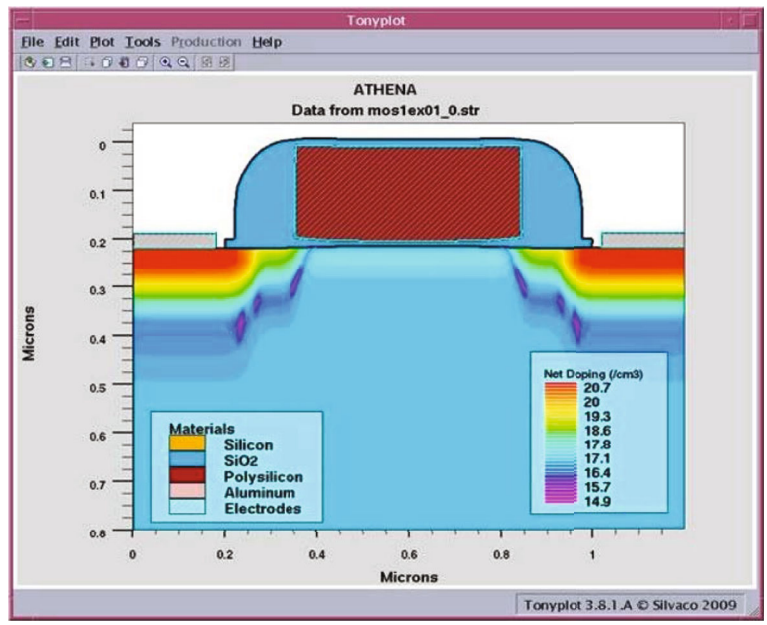

Figure 22: Silvaco graphical user interface for solar cell simulation [251].

affect the device including wide-bandgap power semiconductors [252]. The researcher may have to find out the source of device failure in order to develop a physical grasp of the device performance [253–255].

6.2.1. TCAD Silvaco Simulation of Epitaxial Structures and Wafer Design. The four polytype hexagonal silicon carbide (4H-SiC) has been selected in designing epitaxial structures. One of the easiest materials to grow or buy in the market is 4H-SiC. The SiC/SiO_2 interface can lead to poor-quality SiC/SiC surface being used as a sensor surface rather than SiO_2/SiC [256]. Silvaco graphical user interface is illustrated in Figure 22, whereas the ATLAS simulation methodology scheme is presented in Figure 23.

6.3. WxAMPS Simulation Method. A 1D solar cell simulation program called widget that provides the analysis of microelectronic and photonic structures (wxAMPS) was developed by the Nankai University of China and the University of Illinois at Urbana-Champaign [257]. This numerical simulation method adheres to the analysis of microelectronic and photonic structures (AMPS) physical concept, adds the share of tunneling currents, enhances convergence and speed, and gives better visualization options.

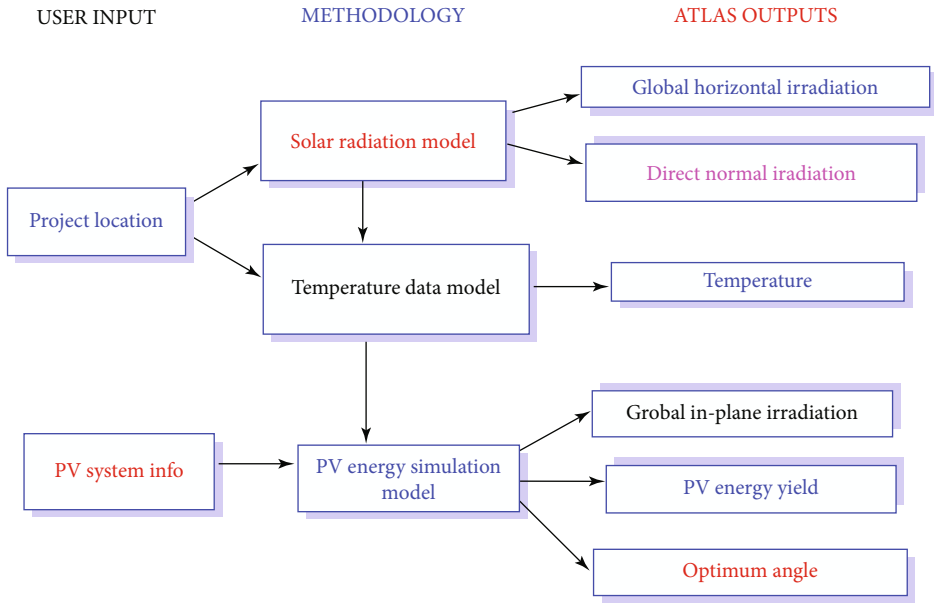

Figure 23: A summary of the ATLAS simulation methodology scheme [251].

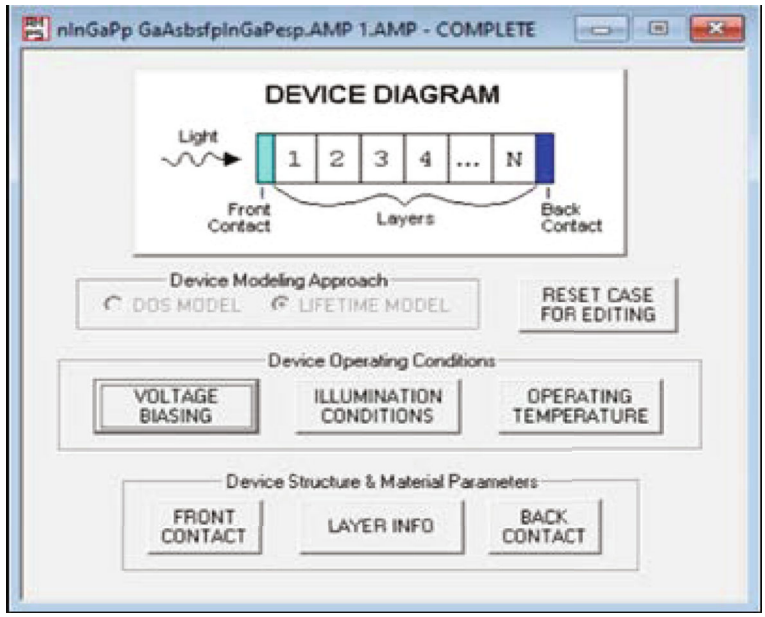

Figure 24: Graphical user interphase for wxAMPS simulation method [257].

The kernel of wxAMPS is based on the upgraded version of AMPS code, while the user interface was created using the cross-platform library wxWidgets [258]. The performance of solar cells is numerically analyzed using the wxAMPS tool. The numerical operation is to solve the Poisson equation which connects charge and electrostatic potential in addition to the hole and electron continuity equations, which represents the behavior of the device. Figure 24 represents the user graphical interface for the wxAMPS simulation software. In wxAMPS, the simulation procedure is undertaken in three steps: first, the ambient operational environment, including temperature, solar spectrum, and bias voltages is set up in which standard values can be fed or the operator can adjust the data accordingly [259]. Secondly, the material properties of the device are entered for each layer. These are provided through a database, editable using common spreadsheet programs, simplifying entering data for many layers and for quick manipulation of properties such as absorption coefficient. After the simulation is initialized, the output is provided in a variety of forms, including files readable by both spreadsheet programs and directly through the graphical user interface [259].

To better simulate different types of solar cells, wxAMPS integrates two alternative tunneling models—the intraband

tunneling framework which supports realistic properties in heterojunction solar cells and the drift-diffusion model. Trap-assisted tunneling current is a key component for tunneling recombination at junctions. Moreover, a new technique that combines the Newton–Raphson approach with the Gummel iteration method has been employed to improve the overall convergence property of the model [260]. Several model outcomes of the simulation are compared in order to obtain the best output parameters to be used in designing high-performance practical cells [261]. Therefore, a solar cell engineer can choose the available model to use for a particular set of materials such as organic or inorganic materials.

7. The Future Outlook of Perovskite Solar Cells

Empowering green energy to reach its full potential is essential in addressing the growing environmental problems the world is facing today as a result of increased pollution occasioned by the use fossil fuels and woody biomass [262]. The utilization of pure renewable sources of energy has gained traction in the advancement of human civilization. Solar energy is perhaps one of the most promising new energy options out of the many available possibilities including nuclear and wind power [263]. Poor stability, despite the fact that power conversion efficiency has so far reached 25.8%, is one of the main obstacles impeding full commercialization of perovskite solar cells (PSCs) [264]. Researchers from all over the world have used a variety of strategies, including structural modification as well as fabrication procedures, in a variety of ways to ensure the needed level of stability and optimal performance are attained. Various factors such as high efficiency, simple manufacture, low cost, and stability are a key component in the commercialization of PSCs. Nevertheless, because different experiments use different testing protocols such as humidity and temperature as well as encapsulation techniques, the stability results offered by diverse researchers cannot be accurately compared [264]. In contrast to stability-related features including lifetime and deterioration rates, PCE is a well-defined metric that can be validated in accordance with set standards. It is also imperative to standardize the necessary test conditions for PSC stability testing, with a focus on elastic modulus, heat resistance, device hysteresis, as well as stability on exposure to light, moisture, and oxygen for each fabrication procedure. It should be understood that although inorganic solar cell test findings have methodologies that have been authorized, they are not frequently used in the analysis of PSC stability. In order to successfully advance PSCs and meet market demands, Research and Development (R&D) goals should be stated [265].

The key challenge in designing very efficient solar cells has been the choice of a robust absorber layer (perovskite), poor device structural engineering, inappropriate band alignment at the absorber interface, as well as carrier recombination at the rear and front contact of the device, which hinders the performance parameters of open circuit voltage V_{oc}, J_{sc}, FF, and PCE [266]. However, more recently, most of the researchers have shown interest in iron disilicide- ($FeSi_2$-) based solar cells because it is an excellent and promising light-absorbing material for solar cell applications owing to its remarkable characteristics such as direct band gap energy of 0.80-0.87 eV, optical absorption coefficient (α) greater than $1 \times 10^5\ cm^{-1}$ at photon energies above 1 eV, which is ~200 times larger than that of crystalline silicon (c-Si) [266]. Moreover, it is chemically stable, highly resistant against environmental and chemical degradation, humidity, oxidation, cosmic rays, radioactive exposures, and high-thermoelectric power coefficient of $k \sim 10^{-4}/K$, and has a large diffusion length of about 38 μm [266]. The $FeSi_2$ photoactive layer is considered binary, nontoxic, and abundant semiconducting material since the forming elements, both Fe and Si, are ecofriendly and mostly available on the earth's crust. According to Ali et al. [267], a numerical simulation of a solar cell architecture based on $FeSi_2$ and PEDOT:PSS HTM gave a remarkable power conversion efficiency of 39.44%. Therefore, with the appropriate device engineering, proper band alignment, and proper fabrication approach, a PCE greater than the S-Q limit should be achievable for practical applications.

Three-dimensional perovskites have driven the remarkable development of organic-inorganic halide perovskite solar cells (PSCs) over the past ten years [268]. Nonetheless, the uncertainty surrounding the stability of 3-D PSCs casts some doubt on their practical performances. Some improvement in the stability of 3D perovskite devices has been made by utilizing several technological and scientific approaches [269]. However, enhancing the halide perovskite's intrinsic chemical stability is the most effective method. On the other hand, 2D perovskites exhibit exceptional stability in ambient circumstances and have been accepted as an alternative to their 3D counterparts [270]. Although the photovoltaic performance of the first generation 2D PSCs has been rather subpar, new findings indicate that they are also capable of generating high PCE levels above 20% [271]. PSCs can be significantly shielded by well-developed encapsulation techniques against exposure and other degrading conditions such as oxygen, moisture, and UV radiation [272]. To achieve the full potential of PSCs, it is essential to have an understanding of the causes of their inherent instability and how to address them. The internal elements that contribute to PSC deterioration such as compositional and phase segregation are linked to transformation in the interfaces of the multiple stacked layers of PSCs and are therefore responsible for their mechanistic degradation. Finally, the momentum to study PSCs should be enhanced, and it would lead to an important breakthrough if flexible tandem solar cell structures are considered more seriously [273]. This could improve device performance while taking into account increased mechanical stability [274]. A study on the robustness of tandem cells in contrast to single junction cells and whether the advantages of flexible photovoltaics are exclusive would be of special interest in the future commercialization of PSCs.

8. Conclusions

The performance of PSC devices has not yet been fully explored with regard to the variety of topologies, fabrication techniques, perovskite compositions, and charge selective layers that have been proposed for better solar cell

performance. To boost the efficiency of PSCs, better light management can be used to reduce light loss from the cell by utilizing transparent conducting oxide layers to minimize absorption losses and silicon oxide layers to harvest more photon energy. Despite the toxic nature of lead, tin–lead halide perovskite's ability to serve as both a light harvester and a hole conductor in the photovoltaic panel is one of its special qualities in device application. Due to their exceptional qualities, such as a tunable bandgap, remarkable defect tolerance, prolonged exciton diffusion range, high carrier mobility, and better absorption coefficient, organometallic lead halides perovskites are potential materials for solar cells. However, their operational lifetimes are constrained as a result of the organic components' susceptibility to environmental degradation. In the recent past, metal halide perovskites have attracted interest as semiconductor devices that achieve desirable properties for optoelectronic application; however, two major challenges, instability and the toxic nature of Pb, remain unaddressed. For this reason, lead-free double perovskites (LFDPs) are emerging as the preferred photoactive absorbers because of their promising PV properties such as intrinsic chemical stability and environmental friendliness. Accordingly, lead-free double perovskites have redefined photovoltaic research despite the fact that a detailed study of their optical, excitonic, and transport characteristics is yet to be understood. Organic-inorganic hybrid PSCs have recently attracted a lot of interest in the photovoltaic community, but recent research has indicated that a missing hydrogen occasioned by poor stability can cause massive energy losses and may therefore be unreliable in the long term. A promising low-cost alternative to current photovoltaic technologies such as crystalline silicon and thin inorganic films is quantum-dot-sensitized solar cells (QDSCs). Quantum dots (QDs) could be made using low-cost techniques, and their size can be adjusted to customize their absorption spectrum. Theoretically, the quantum dot solar cell (QDSC) has been determined to achieve a theoretical PCE of up to 66% due to the occurrence of a unique phenomenon referred to as multiexciton production. However, the experimental values of PCE for QDSCs are quite low compared to what is theoretically predicted. Nonetheless, one of the most desirable QDs is PbS colloidal quantum dots (QDs), which have received significant interest as promising building blocks for optoelectronic devices because of their size-dependent band gap and tunability of electronic properties by means of surface chemistry and solution processability. Although many organic HTMs have been fabricated with satisfactory efficiency, it is still unclear how molecule shape affects how well HTMs work. Metal back contacts in photovoltaic cells should result in the design of low-cost, chemically resistant, and easily processed and fabricated photovoltaic cells. The back contact of a PV cell is essential to ensuring effective charge transport to the cell's external circuit. Compositional engineering will be the main strategy because this will considerably increase perovskite lattice entropy. Additionally, the various film deposition procedures, component engineering of an all-inorganic perovskite materials, and energy loss mechanisms are essential. In this regard, researchers have successfully used a variety of approaches, including solution-processing and coevaporation techniques, to improve film quality with optimal grain size and uniform coverage. The deposition parameters, including evaporation rate, solvents, and temperature, have a significant impact on the dynamics of crystallization. To properly adjust the deposition settings and produce pinhole-free, smooth, and big grain-size films, more studies on the kinetics of crystallization are essential. The long-term operational stability of inorganic PSCs is proposed to receive considerable interest in the future because they are cost-effective to fabricate and have the potential to post remarkable power conversation efficiency. The use of numerical analysis of perovskite solar cells to investigate interface engineering and overall device performance has been presented. The simulation features of various computational strategies such as SCAPS-1D, Silvaco ATLAS, and WxAMPS with regard to perovskite solar cells are critical in the design of solar cells with high performance. The simulation tools herein discussed have gained traction in guiding the fabrication of practical solar cells that can be introduced into the production workflow for commercial applications.

Data Availability

The data associated with the findings of this study are available from the corresponding author upon reasonable request.

Consent

This article has the consent of all the authors.

Conflicts of Interest

The authors have no competing interests

Authors' Contributions

GGN did the analysis, writing, and editing. JKK performed the method development, editing, and supervision. All authors have read and approved the manuscript.

Acknowledgments

The authors are grateful to the Department of Chemistry and Directorate of Research, Egerton University, Njoro Campus, for supporting this study.

References

[1] M. Takase, R. Kipkoech, and P. K. Essandoh, "A comprehensive review of energy scenario and sustainable energy in Kenya," *Fuel Communications*, vol. 7, article 100015, 2021.

[2] L. Kong, Z. Yuan, N. Sun et al., "Advances in flexible hydrogels for light-thermal-electricity energy conversion and storage," *Journal of Energy Storage*, vol. 60, article 106618, 2023.

[3] P. Roy, A. Ghosh, F. Barclay, A. Khare, and E. Cuce, "Perovskite solar cells: a review of the recent advances," *Coatings*, vol. 12, no. 8, p. 1089, 2022.

[4] A. Fakharuddin, M. Vasilopoulou, A. Soultati et al., "Robust inorganic hole transport materials for organic and perovskite solar cells: insights into materials electronic properties and device performance," *Solar RRL*, vol. 5, no. 1, article 2000555, 2021.

[5] S. Sarker, M. T. Islam, A. Rauf et al., "A simulation based incremental study of stable perovskite-on-perovskite tandem solar device utilizing non-toxic tin and germanium perovskite," *Materials Today Communications*, vol. 32, article 103881, 2022.

[6] A. M. Elseman, C. Xu, Y. Yao et al., "Electron transport materials: evolution and case study for high-efficiency perovskite solar cells," *Solar RRL*, vol. 4, no. 7, article 2000136, 2020.

[7] M. A. Green, A. Ho-Baillie, and H. J. Snaith, "The emergence of perovskite solar cells," *Nature Photonics*, vol. 8, no. 7, pp. 506–514, 2014.

[8] H. Min, D. Y. Lee, J. Kim et al., "Perovskite solar cells with atomically coherent interlayers on SnO_2 electrodes," *Nature*, vol. 598, no. 7881, pp. 444–450, 2021.

[9] Z. Guo, A. K. Jena, G. M. Kim, and T. Miyasaka, "The high open-circuit voltage of perovskite solar cells: a review," *Energy & Environmental Science*, vol. 15, no. 8, pp. 3171–3222, 2022.

[10] N. N. Lal, Y. Dkhissi, W. Li, Q. Hou, Y. B. Cheng, and U. Bach, "Perovskite tandem solar cells," *Advanced Energy Materials*, vol. 7, no. 18, article 1602761, 2017.

[11] Z. Liu, S. E. Sofia, H. S. Laine et al., "Revisiting thin silicon for photovoltaics: a technoeconomic perspective," *Energy & Environmental Science*, vol. 13, no. 1, pp. 12–23, 2020.

[12] Y. Li, L. Meng, Y. M. Yang et al., "High-efficiency robust perovskite solar cells on ultrathin flexible substrates," *Nature Communications*, vol. 7, no. 1, pp. 1–10, 2016.

[13] P. Roy, N. K. Sinha, S. Tiwari, and A. Khare, "A review on perovskite solar cells: evolution of architecture, fabrication techniques, commercialization issues and status," *Solar Energy*, vol. 198, pp. 665–688, 2020.

[14] I. Turkevych, S. Kazaoui, N. A. Belich et al., "Strategic advantages of reactive polyiodide melts for scalable perovskite photovoltaics," *Nature Nanotechnology*, vol. 14, no. 1, pp. 57–63, 2019.

[15] H. Aljaghoub, F. Abumadi, M. N. AlMallahi, K. Obaideen, and A. H. Alami, "Solar PV cleaning techniques contribute to Sustainable Development Goals (SDGs) using multi-criteria decision-making (MCDM): assessment and review," *International Journal of Thermofluids*, vol. 16, article 100233, 2022.

[16] D. Cheng, Z. Yang, and Y. Liang, "Preparation and energy storage performance of perovskite luminescent materials by an electrochemiluminescence method," *Adsorption Science & Technology*, vol. 2022, Article ID 3092941, 10 pages, 2022.

[17] P. P. Khirade and A. V. Raut, "Perovskite structured materials: synthesis, structure, physical properties and applications," in *Recent Advances in Multifunctional Perovskite Materials*, IntechOpen, 2022.

[18] G. Grancini and M. K. Nazeeruddin, "Dimensional tailoring of hybrid perovskites for photovoltaics," *Nature Reviews Materials*, vol. 4, no. 1, pp. 4–22, 2019.

[19] J. Zhou, X. Su, Q. Huang et al., "Recent advancements in poly-Si/SiO_x passivating contacts for high-efficiency silicon solar cells: technology review and perspectives," *Journal of Materials Chemistry A*, vol. 10, no. 38, pp. 20147–20173, 2022.

[20] T. Gao, Q. Yang, X. Guo et al., "An industrially viable TOPCon structure with both ultra-thin SiO_x and n^+-poly-Si processed by PECVD for p-type c-Si solar cells," *Solar Energy Materials and Solar Cells*, vol. 200, article 109926, 2019.

[21] Z. Fang, Q. Zeng, C. Zuo et al., "Perovskite-based tandem solar cells," *Science Bulletin*, vol. 66, no. 6, pp. 621–636, 2021.

[22] A. Mohammadnia, A. Rezania, B. M. Ziapour, F. Sedaghati, and L. Rosendahl, "Hybrid energy harvesting system to maximize power generation from solar energy," *Energy Conversion and Management*, vol. 205, article 112352, 2020.

[23] J. Chaudhary, S. Choudhary, C. M. S. Negi, S. K. Gupta, and A. S. Verma, "Surface morphological, optical and electrical characterization of methylammonium lead bromide perovskite (CH3NH3PbBr3) thin film," *Physica Scripta*, vol. 94, no. 10, article 105821, 2019.

[24] A. Husainat, W. Ali, P. Cofie, J. Attia, J. Fuller, and A. Darwish, "Simulation and analysis method of different back metals contact of $CH_3NH_3PbI_3$ perovskite solar cell along with electron transport layer TiO₂ using MBMT-MAPLE/PLD," *American Journal of Optics and Photonics*, vol. 8, no. 1, pp. 6–26, 2020.

[25] P. Su, Y. Liu, J. Zhang et al., "Pb-based perovskite solar cells and the underlying pollution behind clean energy: Dynamic leaching of toxic substances from discarded perovskite solar cells," *The Journal of Physical Chemistry Letters*, vol. 11, no. 8, pp. 2812–2817, 2020.

[26] S. P. Singh and P. Nagarjuna, "Organometal halide perovskites as useful materials in sensitized solar cells," *Dalton Transactions*, vol. 43, no. 14, pp. 5247–5251, 2014.

[27] U. Mandadapu, S. V. Vedanayakam, and K. Thyagarajan, "Simulation and analysis of lead based perovskite solar cell using SCAPS-1D," *Indian Journal of Science and Technology*, vol. 10, pp. 65–72, 2017.

[28] W. Ke, G. Fang, Q. Liu et al., "Low-temperature solution-processed tin oxide as an alternative electron transporting layer for efficient perovskite solar cells," *Journal of the American Chemical Society*, vol. 137, no. 21, pp. 6730–6733, 2015.

[29] D. Liu, M. K. Gangishetty, and T. L. Kelly, "Effect of CH3NH3PbI3thickness on device efficiency in planar heterojunction perovskite solar cells," *Journal of Materials Chemistry A*, vol. 2, no. 46, pp. 19873–19881, 2014.

[30] S. Ye, W. Sun, Y. Li et al., "CuSCN-based inverted planar perovskite solar cell with an average PCE of 15.6%," *Nano Letters*, vol. 15, no. 6, pp. 3723–3728, 2015.

[31] Q. Fu, X. Tang, B. Huang et al., "Recent progress on the long-term stability of perovskite solar cells," *Advanced Science*, vol. 5, no. 5, article 1700387, 2018.

[32] Z. Li, T. R. Klein, D. H. Kim et al., "Scalable fabrication of perovskite solar cells," *Nature Reviews Materials*, vol. 3, no. 4, pp. 1–20, 2018.

[33] M. Ren, X. Qian, Y. Chen, T. Wang, and Y. Zhao, "Potential lead toxicity and leakage issues on lead halide perovskite photovoltaics," *Journal of Hazardous Materials*, vol. 426, article 127848, 2022.

[34] N. K. Noel, S. D. Stranks, A. Abate et al., "Lead-free organic–inorganic tin halide perovskites for photovoltaic applications," *Energy & Environmental Science*, vol. 7, pp. 3061–3068, 2014.

[35] M. Wang, W. Wang, B. Ma et al., "Lead-free perovskite materials for solar cells," *Nano-Micro Letters*, vol. 13, p. 62, 2021.

[36] F. De Angelis, D. Meggiolaro, E. Mosconi, A. Petrozza, M. K. Nazeeruddin, and H. J. Snaith, "Trends in perovskite solar cells and optoelectronics: status of research and applications from the PSCO conference," *ACS Energy Letters*, vol. 2, no. 4, pp. 857–861, 2017.

[37] M. S. Mani, M. B. Joshi, R. R. Shetty et al., "Lead exposure induces metabolic reprogramming in rat models," *Toxicology Letters*, vol. 335, pp. 11–27, 2020.

[38] Q. Cao, T. Wang, J. Yang et al., "Environmental-friendly polymer for efficient and stable inverted perovskite solar cells with mitigating lead leakage," *Advanced Functional Materials*, vol. 32, no. 32, article 2201036, 2022.

[39] W. Ke and M. G. Kanatzidis, "Prospects for low-toxicity lead-free perovskite solar cells," *Nature Communications*, vol. 10, no. 1, pp. 1–4, 2019.

[40] X. Liu, T. Wu, X. Luo et al., "Lead-free perovskite solar cells with over 10% efficiency and size 1 cm2 enabled by solvent–crystallization regulation in a two-step deposition method," *ACS Energy Letters*, vol. 7, pp. 425–431, 2022.

[41] A. Bibi, I. Lee, Y. Nah et al., "Lead-free halide double perovskites: toward stable and sustainable optoelectronic devices," *Materials Today*, vol. 49, pp. 123–144, 2021.

[42] X. Li, J. Shi, J. Chen, Z. Tan, and H. Lei, "Lead-free halide double perovskite for high-performance photodetectors: progress and perspective," *Materials*, vol. 16, no. 12, p. 4490, 2023.

[43] H. Tang, Y. Xu, X. Hu et al., "Lead-free halide double perovskite nanocrystals for light-emitting applications: strategies for boosting efficiency and stability," *Advanced Science*, vol. 8, article 2004118, 2021.

[44] X. Zhang, M. E. Turiansky, and C. G. Van de Walle, "All-inorganic halide perovskites as candidates for efficient solar cells," *Cell Reports Physical Science*, vol. 2, article 100604, 2021.

[45] M. Jain, P. Bhumla, M. Kumar, and S. Bhattacharya, "Lead-free alloyed double perovskites: an emerging class of materials for optoelectronic applications," *The Journal of Physical Chemistry C*, vol. 126, pp. 6753–6760, 2022.

[46] S. Ghosh, H. Shankar, and P. Kar, "Recent developments of lead-free halide double perovskites: a new superstar in the optoelectronic field," *Materials Advances*, vol. 3, pp. 3742–3765, 2022.

[47] P.-K. Kung, M.-H. Li, P.-Y. Lin et al., "Lead-free double perovskites for perovskite solar cells," *Solar RRL*, vol. 4, no. 2, article 1900306, 2020.

[48] S. Rai, B. Pandey, A. Garg, and D. Dwivedi, "Hole transporting layer optimization for an efficient lead-free double perovskite solar cell by numerical simulation," *Optical Materials*, vol. 121, article 111645, 2021.

[49] M. H. Li, J. Y. Shao, Y. Jiang et al., "Electrical loss management by molecularly manipulating dopant-free Poly(3-hexylthiophene) towards 16.93% CsPbI2Br solar cells," *Angewandte Chemie*, vol. 133, no. 30, pp. 16524–16529, 2021.

[50] N. Singh, A. Agarwal, and M. Agarwal, "Performance evaluation of lead-free double-perovskite solar cell," *Optical Materials*, vol. 114, article 110964, 2021.

[51] H. Yan, B. Wang, X. Yan et al., "Efficient passivation of surface defects by lewis base in lead-free tin-based perovskite solar cells," *Materials Today Energy*, vol. 27, article 101038, 2022.

[52] T. Wu, X. Liu, X. Luo et al., "Lead-free tin perovskite solar cells," *Joule*, vol. 5, pp. 863–886, 2021.

[53] C. Wu, Q. Zhang, Y. Liu et al., "The dawn of lead-free perovskite solar cell: highly stable double perovskite Cs2AgBiBr6-Film," *Advanced Science*, vol. 5, no. 3, article 1700759, 2018.

[54] H. Liu, Z. Zhang, W. Zuo et al., "Pure tin halide perovskite solar cells: focusing on preparation and strategies," *Advanced Energy Materials*, vol. 13, no. 3, article 2202209, 2023.

[55] X. Wang, T. Zhang, Y. Lou, and Y. Zhao, "All-inorganic lead-free perovskites for optoelectronic applications," *Materials Chemistry Frontiers*, vol. 3, pp. 365–375, 2019.

[56] A. Abate, "Perovskite solar cells go lead free," *Joule*, vol. 1, no. 4, pp. 659–664, 2017.

[57] N. Marinova, S. Valero, and J. L. Delgado, "Organic and perovskite solar cells: working principles, materials and interfaces," *Journal of Colloid and Interface Science*, vol. 488, pp. 373–389, 2017.

[58] W. Li, Z. Wang, F. Deschler, S. Gao, R. H. Friend, and A. K. Cheetham, "Chemically diverse and multifunctional hybrid organic-inorganic perovskites," *Nature Reviews Materials*, vol. 2, no. 3, pp. 1–18, 2017.

[59] X. Liu, X. Du, J. Wang et al., "Efficient organic solar Cells with extremely high open-circuit voltages and low voltage losses by suppressing nonradiative recombination Losses," *Advanced Energy Materials*, vol. 8, no. 26, article 1801699, 2018.

[60] M. Wright and A. Uddin, "Organic–inorganic hybrid solar cells: A comparative review," *Solar Energy Materials and Solar Cells*, vol. 107, pp. 87–111, 2012.

[61] S. A. Kandjani, S. Mirershadi, and A. Nikniaz, "Inorganic–organic perovskite solar cells," *Solar Cells-New Approaches and Reviews*, vol. 10, article 58970, 2015.

[62] J. Wang, J. Zhang, Y. Zhou et al., "Highly efficient all-inorganic perovskite solar cells with suppressed non-radiative recombination by a Lewis base," *Nature Communications*, vol. 11, p. 177, 2020.

[63] K. Sanglee, M. Nukunudompanich, F. Part et al., "The current state of the art in internal additive materials and quantum dots for improving efficiency and stability against humidity in perovskite solar cells," *Heliyon*, vol. 8, no. 12, article e11878, 2022.

[64] F. Khan, B. D. Rezgui, M. T. Khan, and F. Al-Sulaiman, "Perovskite-based tandem solar cells: device architecture, stability, and economic perspectives," *Renewable and Sustainable Energy Reviews*, vol. 165, article 112553, 2022.

[65] S. Akhil, S. Akash, A. Pasha et al., "Review on perovskite silicon tandem solar cells: Status and prospects 2T, 3T and 4T for real world conditions," *Materials & Design*, vol. 211, article 110138, 2021.

[66] J. L. Prasanna, E. Goel, A. Kumar et al., "Bandgap graded perovskite solar cell for above 30% efficiency," *Optik*, vol. 269, article 169891, 2022.

[67] L. Liu, H. Xiao, K. Jin et al., "4-Terminal inorganic perovskite/organic tandem solar cells offer 22% efficiency," *Nano-Micro Letters*, vol. 15, no. 1, p. 23, 2023.

[68] A. Razzaq, T. G. Allen, W. Liu, Z. Liu, and S. De Wolf, "Silicon heterojunction solar cells: Techno-economic assessment and opportunities," *Joule*, vol. 6, no. 3, pp. 514–542, 2022.

[69] A. Rajagopal, Z. Yang, S. B. Jo et al., "Highly efficient perovskite–perovskite tandem solar cells reaching 80% of the theoretical limit in photovoltage," *Advanced Materials*, vol. 29, no. 34, article 1702140, 2017.

[70] Y. Wang, S. Gu, G. Liu et al., "Cross-linked hole transport layers for high-efficiency perovskite tandem solar cells," *Science China Chemistry*, vol. 64, pp. 2025–2034, 2021.

[71] L. Gil-Escrig, S. Hu, K. P. Zanoni et al., "Perovskite/perovskite tandem solar cells in the substrate configuration with potential for bifacial operation," *ACS Materials Letters*, vol. 4, no. 12, pp. 2638–2644, 2022.

[72] H. Sun, K. Deng, J. Xiong, and L. Li, "Graded bandgap perovskite with intrinsic n–p homojunction expands photon harvesting range and enables all transport layer-free perovskite solar cells," *Advanced Energy Materials*, vol. 10, no. 8, article 1903347, 2020.

[73] M. Bacha, A. Saadoune, I. Youcef, and O. terghini, "Design and numerical investigation of perovskite/silicon tandem solar cell," *Optical Materials*, vol. 131, article 112671, 2022.

[74] K. Amri, R. Belghouthi, M. Aillerie, and R. Gharbi, "Device optimization of a lead-free perovskite/silicon tandem solar cell with 24.4% power conversion efficiency," *Energies*, vol. 14, no. 12, p. 3383, 2021.

[75] M. Xiaohui, Y. Liqun, Z. Shijian, D. Qilin, C. Cong, and S. Hongwei, "All-inorganic perovskite solar cells: status and future," *Progress in Chemistry*, vol. 32, p. 1608, 2020.

[76] H. Zhong, W. Li, Y. Huang et al., "All-Inorganic perovskite solar cells with tetrabutylammonium acetate as the buffer layer between the SnO2Electron transport film and CsPbI3," *ACS Applied Materials & Interfaces*, vol. 14, no. 4, pp. 5183–5193, 2022.

[77] N. A. N. Ouedraogo, Y. Chen, Y. Y. Xiao et al., "Stability of all-inorganic perovskite solar cells," *Nano Energy*, vol. 67, article 104249, 2020.

[78] A. Bashir and M. Sultan, "Organometal halide perovskite-based materials and their applications in solar cell devices," in *Solar Cells: From Materials to Device Technology*, S. K. Sharma and K. Ali, Eds., pp. 259–281, Springer International Publishing, Cham, Switzerland, 2020.

[79] C. Quarti, C. Katan, and J. Even, "Physical properties of bulk, defective, 2D and 0D metal halide perovskite semiconductors from a symmetry perspective," *Journal of Physics: Materials*, vol. 3, no. 4, article 042001, 2020.

[80] F. Kong and S. Dai, "Chapter 3 The dyes used in dye-sensitized solar cells," *Dye-sensitized Solar Cells*, vol. 7, p. 139, 2022.

[81] Q. I. Qasim and Q. I. Qasim, "The influence of the SWOT analysis strategy on the achievement of the fifth preparatory literary class students' evaluative thinking at history," *International Journal of Early Childhood Special Education (INTJECSE)*, vol. 13, no. 2, pp. 66–78, 2021.

[82] N. Lakhdar and A. Hima, "Electron transport material effect on performance of perovskite solar cells based on CH3NH3GeI3," *Optical Materials.*, vol. 99, article 109517, 2020.

[83] A. Hima, N. Lakhdar, B. Benhaoua, A. Saadoune, I. Kemerchou, and F. Rogti, "An optimized perovskite solar cell designs for high conversion efficiency," *Superlattices and Microstructures*, vol. 129, pp. 240–246, 2019.

[84] X. Wei, X. Wang, H. Jiang et al., "Numerical simulation and experimental validation of inverted planar perovskite solar cells based on NiOx hole transport layer," *Superlattices and Microstructures*, vol. 112, pp. 383–393, 2017.

[85] I. Qasim, O. Ahmad, Z. ul Abdin et al., "Design and numerical investigations of eco-friendly, non-toxic (Au/CuSCN/CH3NH3SnI3/CdTe/ZnO/ITO) perovskite solar cell and module," *Solar Energy*, vol. 237, pp. 52–61, 2022.

[86] Y. Xu, L. Xie, X. Zhang et al., "Pc-darts: partial channel connections for memory-efficient architecture search," 2019, https://arxiv.org/abs/1907.05737.

[87] S. Rühle, M. Shalom, and A. Zaban, "Quantum-dot-sensitized solar cells," *ChemPhysChem*, vol. 11, no. 11, pp. 2290–2304, 2010.

[88] J. Markna and P. K. Rathod, "Review on the efficiency of quantum dot sensitized solar cell: insights into photoanodes and QD sensitizers," *Dyes and Pigments*, vol. 199, article 110094, 2022.

[89] D.-K. Hwang, H. J. Jo, D.-H. Kim, E. J. Lee, and R. P. Chang, "Hybrid dual-stage flow-synthesis of eco-friendly ZnCuInSSe quantum dots for solar cells: Improvement in efficiency using inorganic ligand exchange," *Journal of Power Sources*, vol. 555, article 232344, 2023.

[90] M. B. Rodhuan, R. A. Kahar, H. N. M. Yazid, A. N. M. Rapi, N. H. Baharin, and N. Burhan, "Size dependency of CdSe for light harvesting in quantum dots solar cell using COMSOL multiphysics," *International Journal of Application on Sciences, Technology and Engineering*, vol. 1, pp. 234–242, 2023.

[91] M. A. Basit, M. A. Ali, Z. Masroor, Z. Tariq, and J. H. Bang, "Quantum dot-sensitized solar cells: a review on interfacial engineering strategies for boosting efficiency," *Journal of Industrial and Engineering Chemistry*, vol. 120, pp. 1–26, 2023.

[92] P. Dubey, B. Pandey, and D. Dwivedi, "Contribution towards the selection of electron and hole transport layers for the development of highly efficient PbS colloidal quantum dot solar cell," *Optik*, vol. 266, article 169600, 2022.

[93] M. A. Rahman, "Design and simulation of a high-performance Cd-free Cu2SnSe3 solar cells with SnS electron-blocking hole transport layer and TiO2 electron transport layer by SCAPS-1D," *SN Applied Sciences*, vol. 3, no. 2, pp. 1–15, 2021.

[94] P. Du, D. Egaña-Ugrinovic, R. Essig, and M. Sholapurkar, "Doped semiconductor devices for sub-MeV dark matter detection," 2022, https://arxiv.org/abs/2212.04504.

[95] Z. Yao, C. Jiang, X. Wang et al., "Recent developments of quantum dot materials for high speed and ultrafast lasers," *Nanomaterials*, vol. 12, no. 7, p. 1058, 2022.

[96] Z. Chen, Q. Su, Z. Qin, and S. Chen, "Effect and mechanism of encapsulation on aging characteristics of quantum-dot light-emitting diodes," *Nano Research*, vol. 14, no. 1, pp. 320–327, 2021.

[97] P. M. Lam, J. Wu, S. Hatch et al., "Effect of rapid thermal annealing on InAs/GaAs quantum dot solar cells," *IET Optoelectronics*, vol. 9, no. 2, pp. 65–68, 2015.

[98] M. Albaladejo-Siguan, E. C. Baird, D. Becker-Koch, Y. Li, A. L. Rogach, and Y. Vaynzof, "Stability of quantum dot solar cells: a matter of (life) time," *Advanced Energy Materials*, vol. 11, no. 12, article 2003457, 2021.

[99] M. Han, O. Karatum, and S. Nizamoglu, "Optoelectronic neural interfaces based on quantum dots," *ACS Applied Materials & Interfaces*, vol. 14, pp. 20468–20490, 2022.

[100] N. Sukharevska, D. Bederak, V. M. Goossens et al., "Scalable PbS quantum dot solar cell production by blade coating from stable inks," *ACS Applied Materials & Interfaces*, vol. 13, pp. 5195–5207, 2021.

[101] Y. Tang, Y. Zhao, and H. Liu, "Room-temperature semiconductor gas sensors: challenges and opportunities," *ACS Sensors*, vol. 7, no. 12, pp. 3582–3597, 2022.

[102] S. Ma, G. Yuan, Y. Zhang, N. Yang, Y. Li, and Q. Chen, "Development of encapsulation strategies towards the commercialization of perovskite solar cells," *Energy & Environmental Science*, vol. 15, no. 1, pp. 13–55, 2022.

[103] J. Yang, J. Lee, J. Lee, and W. Yi, "Suppressed interfacial charge recombination of PbS quantum dot photovoltaics by graphene incorporated into ZnO nanoparticles," *ACS Applied Materials & Interfaces*, vol. 10, no. 30, pp. 25311–25320, 2018.

[104] R. Zhou, J. Xu, P. Luo et al., "Near-infrared photoactive semiconductor quantum dots for solar cells," *Advanced Energy Materials*, vol. 11, no. 40, article 2101923, 2021.

[105] M. A. Deshmukh, S.-J. Park, B. S. Hedau, and T.-J. Ha, "Recent progress in solar cells based on carbon nanomaterials," *Solar Energy*, vol. 220, pp. 953–990, 2021.

[106] D. Liu, K. Kim, J. Kim, J. Gong, T.-H. Chang, and Z. Ma, *Novel Materials-Based Flexible Solar Cells*, Inorganic Flexible Optoelectronics: Materials and Applications, 2019.

[107] X. Zhang and E. M. Johansson, "Reduction of charge recombination in PbS colloidal quantum dot solar cells at the quantum dot/ZnO interface by inserting a MgZnO buffer layer," *Journal of Materials Chemistry A*, vol. 5, no. 1, pp. 303–310, 2017.

[108] H. Wang, H. Li, W. Cai et al., "Challenges and strategies relating to device function layers and their integration toward high-performance inorganic perovskite solar cells," *Nanoscale*, vol. 12, no. 27, pp. 14369–14404, 2020.

[109] P. Huirong, C. Molang, M. Shuang, S. Xiaoqiang, L. Xuepeng, and D. Songyuan, "Fabrication and stability of all-inorganic perovskite solar cells," *Progress in Chemistry*, vol. 33, p. 136, 2021.

[110] A. Bernasconi, A. Rizzo, A. Listorti et al., "Synthesis, properties, and modeling of Cs1–xRbxSnBr3Solid solution: a new mixed-cation lead-free all-inorganic perovskite system," *Chemistry of Materials*, vol. 31, no. 9, pp. 3527–3533, 2019.

[111] J. Deng, J. Li, Z. Yang, and M. Wang, "All-inorganic lead halide perovskites: a promising choice for photovoltaics and detectors," *Journal of Materials Chemistry C*, vol. 7, no. 40, pp. 12415–12440, 2019.

[112] Y.-Y. Liu, Y. Wang, T. R. Walsh et al., "Emergence of plasmid-mediated colistin resistance mechanism MCR-1 in animals and human beings in China: a microbiological and molecular biological study," *The Lancet Infectious Diseases*, vol. 16, no. 2, pp. 161–168, 2016.

[113] Q. Yang, S. Yang, T. Xi, H. Li, J. Yi, and J. Zhong, "Gradient doping simulation of perovskite solar cells with $CH_3NH_3Sn_{1-x}Pb_xI_3$ as the absorber layer," *Current Applied Physics*, vol. 44, pp. 55–62, 2022.

[114] C. Chen, S. Zheng, and H. Song, "Photon management to reduce energy loss in perovskite solar cells," *Chemical Society Reviews*, vol. 50, no. 12, pp. 7250–7329, 2021.

[115] M. Jošt, B. Lipovšek, B. Glažar et al., "Perovskite solar cells go outdoors: field testing and temperature effects on energy yield," *Advanced Energy Materials*, vol. 10, no. 25, article 2000454, 2020.

[116] L. Zheng, Y. Xuan, J. Wang, S. Bao, X. Liu, and K. Zhang, "Inverted perovskite/silicon V-shaped tandem solar cells with 27.6% efficiencyviaself-assembled monolayer-modified nickel oxide layer," *Journal of Materials Chemistry A*, vol. 10, no. 13, pp. 7251–7262, 2022.

[117] H. Li and W. Zhang, "Perovskite tandem solar cells: from fundamentals to commercial deployment," *Chemical Reviews*, vol. 120, no. 18, pp. 9835–9950, 2020.

[118] V. Tyagi, N. A. Rahim, N. Rahim, A. Jeyraj, and L. Selvaraj, "Progress in solar PV technology: research and achievement," *Renewable and Sustainable Energy Reviews*, vol. 20, pp. 443–461, 2013.

[119] J. Zhou, Q. Huang, Y. Ding, G. Hou, and Y. Zhao, "Passivating contacts for high-efficiency silicon-based solar cells: from single-junction to tandem architecture," *Nano Energy*, vol. 92, article 106712, 2022.

[120] S. Bhattacharya and S. John, "Beyond 30% conversion efficiency in silicon solar cells: a numerical demonstration," *Scientific Reports*, vol. 9, article 12482, 2019.

[121] J. Werner, B. Niesen, and C. Ballif, "Perovskite/silicon tandem solar cells: marriage of convenience or true love story?–An overview," *Advanced Materials Interfaces*, vol. 5, no. 1, article 1700731, 2018.

[122] G. Niu, X. Guo, and L. Wang, "Review of recent progress in chemical stability of perovskite solar cells," *Journal of Materials Chemistry A*, vol. 3, no. 17, pp. 8970–8980, 2015.

[123] M. Asghar, J. Zhang, H. Wang, and P. Lund, "Device stability of perovskite solar cells - A review," *Renewable and Sustainable Energy Reviews*, vol. 77, pp. 131–146, 2017.

[124] Y. I. Lee, N. J. Jeon, B. J. Kim et al., "A low-temperature thin-film encapsulation for enhanced stability of a highly efficient perovskite solar cell," *Advanced Energy Materials*, vol. 8, no. 9, article 1701928, 2018.

[125] Y. Yang, I. Wyatt, D. Travis, and M. Bahorsky, "Decolorization of Dyes Using UV/H 2 O 2 photochemical oxidation," *Textile Chemist & Colorist*, vol. 30, 1998.

[126] J. Heller, T. F. Pascher, D. Muß, C. van der Linde, M. K. Beyer, and M. Ončák, "Photochemistry and UV/vis spectroscopy of hydrated vanadium cations, $V^+(H_2O)_n$, n = 1–41, a model system for photochemical hydrogen evolution," *Physical Chemistry Chemical Physics*, vol. 23, no. 39, pp. 22251–22262, 2021.

[127] B. Philippe, G. J. Man, and H. Rensmo, "Photoelectron spectroscopy investigations of halide perovskite materials used in solar cells," in *Characterization Techniques for Perovskite Solar Cell Materials*, pp. 109–137, Elsevier, 2020.

[128] D. M. Jones, Y. An, J. Hidalgo, C. Evans, J. N. Vagott, and J.-P. Correa-Baena, "Polymers and interfacial modifiers for durable perovskite solar cells: a review," *Journal of Materials Chemistry C*, vol. 9, no. 37, pp. 12509–12522, 2021.

[129] S. S. Mali and C. K. Hong, "p-i-n/n-i-p type planar hybrid structure of highly efficient perovskite solar cells towards improved air stability: synthetic strategies and the role of p-type hole transport layer (HTL) and n-type electron transport layer (ETL) metal oxides," *Nanoscale*, vol. 8, no. 20, pp. 10528–10540, 2016.

[130] Z. Song, S. C. Watthage, A. B. Phillips, and M. J. Heben, "Pathways toward high-performance perovskite solar cells: review of recent advances in organo-metal halide perovskites for photovoltaic applications," *Journal of Photonics for Energy*, vol. 6, no. 2, pp. 022001–022001, 2016.

[131] Y. Yao, C. Cheng, C. Zhang, H. Hu, K. Wang, and S. De Wolf, "Organic hole-transport layers for efficient, stable, and scalable inverted perovskite solar cells," *Advanced Materials*, vol. 34, no. 44, article 2203794, 2022.

[132] Z. Li, J. Park, H. Park et al., "Graded heterojunction of perovskite/dopant-free polymeric hole-transport layer for efficient and stable metal halide perovskite devices," *Nano Energy*, vol. 78, article 105159, 2020.

[133] S. Pitchaiya, M. Natarajan, A. Santhanam et al., "A review on the classification of organic/inorganic/carbonaceous hole transporting materials for perovskite solar cell application," *Arabian Journal of Chemistry*, vol. 13, no. 1, pp. 2526–2557, 2020.

[134] Z. Wang and Y. Jiang, "Advances in perovskite solar cells: film morphology control and interface engineering," *Journal of Cleaner Production*, vol. 317, article 128368, 2021.

[135] M. K. Rao, D. Sangeetha, M. Selvakumar, Y. Sudhakar, and M. Mahesha, "Review on persistent challenges of perovskite solar cells' stability," *Solar Energy*, vol. 218, pp. 469–491, 2021.

[136] F. M. Guangul and G. T. Chala, "Solar energy as renewable energy source: SWOT analysis," in *2019 4th MEC international conference on big data and smart city (ICBDSC)*, pp. 1–5, Muscat, Oman, 2019.

[137] F. H. Alharbi and S. Kais, "Theoretical limits of photovoltaics efficiency and possible improvements by intuitive approaches learned from photosynthesis and quantum coherence," *Renewable and Sustainable Energy Reviews*, vol. 43, pp. 1073–1089, 2015.

[138] M. Omrani, R. Keshavarzi, M. Abdi-Jalebi, and P. Gao, "Impacts of plasmonic nanoparticles incorporation and interface energy alignment for highly efficient carbon-based perovskite solar cells," *Scientific Reports*, vol. 12, no. 1, 2022.

[139] N. Eswaramoorthy and K. Rajaram, "Planar perovskite solar cells: plasmonic nanoparticles-modifiedZnOas an electron transport layer for enhancing the device performance and stability at ambient conditions," *International Journal of Energy Research*, vol. 46, no. 8, pp. 10724–10740, 2022.

[140] T. Hu, K. Dai, J. Zhang, and S. Chen, "Noble-metal-free Ni_2P modified step-scheme $SnNb_2O_6$/CdS-diethylenetriamine for photocatalytic hydrogen production under broadband light irradiation," *Applied Catalysis B: Environmental*, vol. 269, article 118844, 2020.

[141] S. B. Patel, A. H. Patel, and J. V. Gohel, "A novel and cost effective CZTS hole transport material applied in perovskite solar cells," *CrystEngComm*, vol. 20, no. 47, pp. 7677–7687, 2018.

[142] M. R. Azani, A. Hassanpour, and T. Torres, "Benefits, problems, and solutions of silver nanowire transparent conductive electrodes in indium tin oxide (ITO)-free flexible solar cells," *Advanced Energy Materials*, vol. 10, no. 48, article 2002536, 2020.

[143] W. Duan, K. Bittkau, A. Lambertz et al., "Improved infrared light management with transparent conductive oxide/amorphous silicon back reflector in high-efficiency silicon heterojunction solar cells," *Solar RRL*, vol. 5, no. 3, article 2000576, 2021.

[144] A. Kandeal, A. K. Thakur, M. Elkadeem et al., "Photovoltaics performance improvement using different cooling methodologies: a state-of-art review," *Journal of Cleaner Production*, vol. 273, article 122772, 2020.

[145] N. Rono, A. E. Merad, J. K. Kibet, B. S. Martincigh, and V. O. Nyamori, "Simulation of the photovoltaic performance of a perovskite solar cell based on methylammonium lead iodide," *Optical and Quantum Electronics*, vol. 54, no. 5, pp. 1–15, 2022.

[146] D. Saikia, M. Alam, J. Bera, A. Betal, A. N. Gandhi, and S. Sahu, "A first-principles study on ABBr3 (A= Cs, Rb, K, Na; B= Ge, Sn) halide perovskites for photovoltaic applications," 2022, https://arxiv.org/abs/2205.01384.

[147] F. Matebese, R. Taziwa, and D. Mutukwa, "Progress on the synthesis and application of CuSCN inorganic hole transport material in perovskite solar cells," *Materials*, vol. 11, no. 12, p. 2592, 2018.

[148] A. Owens and A. Peacock, "Compound semiconductor radiation detectors," *Nuclear Instruments and Methods in Physics Research Section A: Accelerators, Spectrometers, Detectors and Associated Equipment*, vol. 531, no. 1-2, pp. 18–37, 2004.

[149] M. C. Scharber and N. S. Sariciftci, "Low band gap conjugated semiconducting polymers," *Advanced Materials Technologies*, vol. 6, no. 4, article 2000857, 2021.

[150] G. Chen, J. Chen, W. Pei et al., "Bismuth ferrite materials for solar cells: current status and prospects," *Materials Research Bulletin*, vol. 110, pp. 39–49, 2019.

[151] S. Z. Haider, H. Anwar, and M. Wang, "Theoretical device engineering for high-performance perovskite solar cells using CuSCN as hole transport material boost the efficiency above 25%," *Physica Status Solidi (a).*, vol. 216, no. 11, article 1900102, 2019.

[152] S. Z. Haider, H. Anwar, and M. Wang, "Remarkable performance optimization of inverted p-i-n architecture perovskite solar cell with CZTS as hole transport material," *Physica B: Condensed Matter*, vol. 620, article 413270, 2021.

[153] A. Kheralla and N. Chetty, "A review of experimental and computational attempts to remedy stability issues of perovskite solar cells," *Heliyon*, vol. 7, no. 2, article e06211, 2021.

[154] G. Saianand, P. Sonar, G. J. Wilson et al., "Current advancements on charge selective contact interfacial layers and electrodes in flexible hybrid perovskite photovoltaics," *Journal of Energy Chemistry*, vol. 54, pp. 151–173, 2021.

[155] F. Liu, J. Zhu, J. Wei et al., "Numerical simulation: toward the design of high-efficiency planar perovskite solar cells," *Applied Physics Letters*, vol. 104, no. 25, article 253508, 2014.

[156] H. Wu, Z. Li, F. Zhang, C. Kang, and Y. Li, "Ionic liquids for efficient and stable perovskite solar cells," *Advanced Materials Interfaces*, vol. 9, no. 32, article 2201292, 2022.

[157] T. Niu, W. Zhu, Y. Zhang et al., "D-A-π-A-D-type dopant-free hole transport material for low-cost, efficient, and stable Perovskite solar cells," *Joule*, vol. 5, no. 1, pp. 249–269, 2021.

[158] L. Lin, T. W. Jones, T. C. J. Yang et al., "Inorganic electron transport materials in perovskite solar cells," *Advanced Functional Materials*, vol. 31, no. 5, article 2008300, 2021.

[159] L. Calió, S. Kazim, M. Grätzel, and S. Ahmad, "Hole-transport materials for perovskite solar cells," *Angewandte Chemie International Edition*, vol. 55, no. 47, pp. 14522–14545, 2016.

[160] G. A. Casas, M. A. Cappelletti, A. P. Cédola, B. M. Soucase, and E. L. Peltzer y Blancá, "Analysis of the power conversion efficiency of perovskite solar cells with different materials as hole-transport layer by numerical simulations," *Superlattices and Microstructures*, vol. 107, pp. 136–143, 2017.

[161] H. D. Pham, T. C. J. Yang, S. M. Jain, G. J. Wilson, and P. Sonar, "Development of dopant-free organic hole transporting materials for perovskite solar cells," *Advanced Energy Materials*, vol. 10, no. 13, article 1903326, 2020.

[162] B. K. Korir, J. K. Kibet, and S. M. Ngari, "Computational simulation of a highly efficient hole transport-free dye-sensitized solar cell based on titanium oxide (TiO2) and zinc oxysulfide

(ZnOS) electron transport layers," *Journal of Electronic Materials*, vol. 50, no. 12, pp. 7259–7274, 2021.

[163] L. Huang, J. Huang, R. Peng, and Z. Ge, "Efficient electron transport layer-free perovskite solar cells enabled by discontinuous polar molecular films: a story of new materials and old ideas?," *ACS Sustainable Chemistry & Engineering*, vol. 9, pp. 936–943, 2021.

[164] C. Momblona, L. Gil-Escrig, E. Bandiello et al., "Efficient vacuum deposited p-i-n and n-i-p perovskite solar cells employing doped charge transport layers," *Energy & Environmental Science*, vol. 9, no. 11, pp. 3456–3463, 2016.

[165] S. Laalioui, K. B. Alaoui, H. A. Dads, K. El Assali, B. Ikken, and A. Outzourhit, "Progress in perovskite based solar cells: scientific and engineering state of the art," *Reviews on Advanced Materials Science*, vol. 59, no. 1, pp. 10–25, 2020.

[166] L. Huang, Z. Hu, J. Xu et al., "Efficient planar perovskite solar cells without a high temperature processed titanium dioxide electron transport layer," *Solar Energy Materials and Solar Cells*, vol. 149, pp. 1–8, 2016.

[167] L.-C. Chen and Z.-L. Tseng, "ZnO-based electron transporting layer for perovskite solar cells," in *Nanostructured Solar Cells*, pp. 203–215, IntechOpen, 2017.

[168] S. Bouazizi, W. Tlili, A. Bouich, B. M. Soucase, and A. Omri, "Design and efficiency enhancement of FTO/PC60BM/CsSn0. 5Ge0. 5I3/Spiro-OMeTAD/Au perovskite solar cell utilizing SCAPS-1D Simulator," *Materials Research Express*, vol. 9, no. 9, article 096402, 2022.

[169] S. Ijaz, E. Raza, Z. Ahmad et al., "Numerical simulation to optimize the efficiency of HTM-free perovskite solar cells by ETM engineering," *Solar Energy*, vol. 250, pp. 108–118, 2023.

[170] J. Allen, B. Shu, L. Zhang, U. Das, and S. Hegedus, "Interdigitated back contact silicon hetero-junction solar cells: the effect of doped layer defect levels and rear surface i-layer band gap on fill factor using two-dimensional simulations," in *2011 37th IEEE Photovoltaic Specialists Conference*, pp. 002545–002549, Seattle, WA, USA, 2011.

[171] A. E. Mansour, M. M. Said, S. Dey et al., "Facile doping and work-function modification of few-layer graphene using molecular oxidants and reductants," *Advanced Functional Materials*, vol. 27, no. 7, article 1602004, 2017.

[172] K. B. Nine, M. F. Hossain, and S. A. Mahmood, "Analysis of stable, environment friendly and highly efficient perovskite solar cell," in *TENCON 2019-2019 IEEE Region 10 Conference (TENCON)*, pp. 1825–1828, Kochi, India, 2019.

[173] T. Wang, G.-J. Xiao, R. Sun, L.-B. Luo, and M.-X. Yi, "High efficiency ETM-free perovskite cell composed of CuSCN and increasing gradient CH3NH3PbI3," *Chinese Physics B*, vol. 31, no. 1, article 018801, 2022.

[174] F. Saeed and H. E. Gelani, "Unravelling the effect of defect density, grain boundary and gradient doping in an efficient lead-free formamidinium perovskite solar cell," *Optical Materials*, vol. 124, article 111952, 2022.

[175] B. Mahapatra, R. V. Krishna, Laxmi, and P. K. Patel, "Design and optimization of CuSCN/CH3NH3PbI3/TiO2 perovskite solar cell for efficient performance," *Optics Communications*, vol. 504, article 127496, 2022.

[176] M. A. Shafi, H. Ullah, S. Ullah, L. Khan, S. Bibi, and B. M. Soucase, "Numerical simulation of lead-free Sn-based perovskite solar cell by using SCAPS-1D," *Engineering Proceedings*, vol. 12, p. 92, 2022.

[177] A. Shpatz Dayan and L. Etgar, "Study of electron transport layer-free and hole transport layer-free inverted perovskite solar cells," *Solar RRL*, vol. 6, article 2100578, 2022.

[178] P. Vivo, J. K. Salunke, and A. Priimagi, "Hole-transporting materials for printable perovskite solar cells," *Materials*, vol. 10, no. 9, p. 1087, 2017.

[179] S. Rai, B. Pandey, and D. Dwivedi, "Designing hole conductor free tin-lead halide based all-perovskite heterojunction solar cell by numerical simulation," *Journal of Physics and Chemistry of Solids*, vol. 156, article 110168, 2021.

[180] H.-J. Du, W.-C. Wang, and J.-Z. Zhu, "Device simulation of lead-free CH3NH3SnI3perovskite solar cells with high efficiency," *Chinese Physics B*, vol. 25, no. 10, article 108802, 2016.

[181] D. N. Q. Agha and Q. T. Algwari, "The influence of the conduction band engineering on the perovskite solar cell performance," *Results in Optics*, vol. 9, article 100291, 2022.

[182] A. Bag, R. Radhakrishnan, R. Nekovei, and R. Jeyakumar, "Effect of absorber layer, hole transport layer thicknesses, and its doping density on the performance of perovskite solar cells by device simulation," *Solar Energy*, vol. 196, pp. 177–182, 2020.

[183] S. Aharon, A. Dymshits, A. Rotem, and L. Etgar, "Temperature dependence of hole conductor free formamidinium lead iodide perovskite based solar cells," *Journal of Materials Chemistry A*, vol. 3, no. 17, pp. 9171–9178, 2015.

[184] B. Chang, B. Li, Z. Wang et al., "Efficient bulk defect suppression strategy in FASnI3Perovskite for photovoltaic performance enhancement," *Advanced Functional Materials*, vol. 32, no. 12, article 2107710, 2022.

[185] J. Song, W. Hu, Z. Li, X.-F. Wang, and W. Tian, "A double hole-transport layer strategy toward efficient mixed tin-lead iodide perovskite solar cell," *Solar Energy Materials and Solar Cells*, vol. 207, article 110351, 2020.

[186] E. Raza, Z. Ahmad, M. Asif et al., "Numerical modeling and performance optimization of carbon-based hole transport layer free perovskite solar cells," *Optical Materials*, vol. 125, article 112075, 2022.

[187] A. Mahapatra, S. Kumar, P. Kumar, and B. Pradhan, "Recent progress in perovskite solar cells: challenges from efficiency to stability," *Materials Today Chemistry*, vol. 23, article 100686, 2022.

[188] P. Mahajan, B. Padha, S. Verma et al., "Review of current progress in hole-transporting materials for perovskite solar cells," *Journal of Energy Chemistry*, vol. 68, pp. 330–386, 2022.

[189] X. Kong, Y. Jiang, X. Wu et al., "Dopant-free F-substituted benzodithiophene copolymer hole-transporting materials for efficient and stable perovskite solar cells," *Journal of Materials Chemistry A*, vol. 8, no. 4, pp. 1858–1864, 2020.

[190] D. Meng, J. Xue, Y. Zhao, E. Zhang, R. Zheng, and Y. Yang, "Configurable organic charge carriers toward stable perovskite photovoltaics," *Chemical Reviews*, vol. 122, no. 18, pp. 14954–14986, 2022.

[191] G. Xu, R. Xue, S. J. Stuard et al., "Reducing energy disorder of hole transport layer by charge transfer complex for high performance p–i–n perovskite solar cells," *Advanced Materials*, vol. 33, no. 13, article 2006753, 2021.

[192] M. Vishnuwaran, K. Ramachandran, D. Anand, and V. Ragavendran, "Using low-cost materials for highly efficient eco-friendly formamidinium tin iodide based solar cell

with copper oxide as hole transport material and titanium oxide as electron transport material with different metal contacts," *Ceramics International*, vol. 48, no. 19, pp. 29314–29321, 2022.

[193] B. Baptayev, Y. Tashenov, and M. P. Balanay, "Conjugated polymers as organic electrodes for photovoltaics," in *Organic Electrodes*, pp. 137–153, Springer, 2022.

[194] K. Domanski, J.-P. Correa-Baena, N. Mine et al., "Not all that glitters is gold: metal-migration-induced degradation in perovskite solar cells," *ACS Nano*, vol. 10, pp. 6306–6314, 2016.

[195] A. Guerrero, J. You, C. Aranda et al., "Interfacial degradation of planar lead halide perovskite solar cells," *ACS Nano*, vol. 10, pp. 218–224, 2016.

[196] T. Ibn-Mohammed, S. Koh, I. Reaney et al., "Perovskite solar cells: an integrated hybrid lifecycle assessment and review in comparison with other photovoltaic technologies," *Renewable and Sustainable Energy Reviews*, vol. 80, pp. 1321–1344, 2017.

[197] A. R. Uhl, A. Rajagopal, J. A. Clark et al., "Solution-processed low-bandgap CuIn (S, Se) 2 absorbers for high-efficiency single-junction and monolithic chalcopyrite-perovskite tandem solar cells," *Advanced Energy Materials*, vol. 8, article 1801254, 2018.

[198] P. Kajal, K. Ghosh, and S. Powar, "Manufacturing techniques of perovskite solar cells," in *Applications of Solar Energy*, pp. 341–364, Springer, 2018.

[199] X. Peng, J. Yuan, S. Shen et al., "Perovskite and organic solar cells fabricated by inkjet printing: progress and prospects," *Advanced Functional Materials*, vol. 27, no. 41, article 1703704, 2017.

[200] Z. Chen, P. He, D. Wu et al., "Processing and preparation method for high-quality opto-electronic perovskite film," *Frontiers in Materials*, vol. 8, article 723169, 2021.

[201] M. J. Perez, V. Fthenakis, H. C. Kim, and A. O. Pereira, "Façade–integrated photovoltaics: a life cycle and performance assessment case study," *Progress in Photovoltaics: Research and Applications*, vol. 20, no. 8, pp. 975–990, 2012.

[202] M. Herrando, D. Elduque, C. Javierre, and N. Fueyo, "Life cycle assessment of solar energy systems for the provision of heating, cooling and electricity in buildings: a comparative analysis," *Energy Conversion and Management*, vol. 257, article 115402, 2022.

[203] J. Mitali, S. Dhinakaran, and A. A. Mohamad, "Energy storage systems: a review," *Energy Storage and Saving*, vol. 1, no. 3, pp. 166–216, 2022.

[204] N. Kumar, M. K. Phani, P. Chamoli et al., "Chapter 10 - Nanomaterials for advanced photovoltaic cells," in *Emerging Nanotechnologies for Renewable Energy*, W. Ahmed, M. Booth, and E. Nourafkan, Eds., pp. 239–258, Elsevier, 2021.

[205] Y. Delannoy, "Purification of silicon for photovoltaic applications," *Journal of Crystal Growth*, vol. 360, pp. 61–67, 2012.

[206] K. Wei, S. Yang, X. Wan, W. Ma, J. Wu, and Y. Lei, "Review of silicon recovery and purification from saw silicon powder," *Jom*, vol. 72, pp. 2633–2647, 2020.

[207] R. Ishikawa, K. Ueno, and H. Shirai, "Improved efficiency of methylammonium-free perovskite thin film solar cells by fluorinated ammonium iodide treatment," *Organic Electronics*, vol. 78, article 105596, 2020.

[208] Y. Heider, P. Willmes, V. Huch, M. Zimmer, and D. Scheschkewitz, "Boron and phosphorus containing heterosiliconoids: stable p-and n-doped unsaturated silicon clusters," *Journal of the American Chemical Society*, vol. 141, no. 49, pp. 19498–19504, 2019.

[209] D. Sirbu, F. H. Balogun, R. L. Milot, and P. Docampo, "Layered perovskites in solar cells: structure, optoelectronic properties, and device design," *Advanced Energy Materials*, vol. 11, no. 24, article 2003877, 2021.

[210] Y. Yang, M. T. Hoang, A. Bhardwaj, M. Wilhelm, S. Mathur, and H. Wang, "Perovskite solar cells based self-charging power packs: fundamentals, applications and challenges," *Nano Energy*, vol. 94, article 106910, 2022.

[211] F. F. Villa, "Silicon properties and crystal growth," in *Silicon Sensors and Actuators*, pp. 3–33, Springer, 2022.

[212] M. Sobayel, M. Chowdhury, T. Hossain et al., "Efficiency enhancement of CIGS solar cell by cubic silicon carbide as prospective buffer layer," *Solar Energy*, vol. 224, pp. 271–278, 2021.

[213] V. T. Lukong, K. Ukoba, and T.-C. Jen, "Review of self-cleaning TiO_2 thin films deposited with spin coating," *The International Journal of Advanced Manufacturing Technology*, vol. 122, no. 9-10, pp. 3525–3546, 2022.

[214] D. E. Weidner, "Numerical modeling of the spray/spin coating of the interior of metal beverage cans: complete three-dimensional simulation," *Journal of Coatings Technology and Research*, vol. 19, no. 1, pp. 97–109, 2022.

[215] M. Buonomenna, "Smart composite membranes for advanced wastewater treatments," in *Smart composite coatings and membranes*, pp. 371–419, Elsevier, 2016.

[216] Y. Yan, Y. Yang, M. Liang et al., "Implementing an intermittent spin-coating strategy to enable bottom-up crystallization in layered halide perovskites," *Nature Communications*, vol. 12, p. 6603, 2021.

[217] M. R. Cavallari, L. M. Pastrana, C. D. F. Sosa et al., "Organic thin-film transistors as gas sensors: a review," *Materials*, vol. 14, p. 3, 2020.

[218] H. Zhang, C. Kinnear, and P. Mulvaney, "Fabrication of single-nanocrystal arrays," *Advanced Materials*, vol. 32, no. 18, article 1904551, 2020.

[219] S.-R. Bae, D. Heo, and S. Kim, "Recent progress of perovskite devices fabricated using thermal evaporation method: perspective and outlook," *Materials Today Advances*, vol. 14, article 100232, 2022.

[220] D. M. Mattox and V. Mattox, *Vacuum Coating Technology*, Springer, 2003.

[221] A. Bashir, T. I. Awan, A. Tehseen, M. B. Tahir, and M. Ijaz, "Interfaces and surfaces," *Chemistry of Nanomaterials*, vol. 51-87, 2020.

[222] F. Mathies, H. Eggers, B. S. Richards, G. Hernandez-Sosa, U. Lemmer, and U. W. Paetzold, "Inkjet-printed triple cation perovskite solar cells," *ACS Applied Energy Materials*, vol. 1, no. 5, pp. 1834–1839, 2018.

[223] Z. Li, P. Li, G. Chen et al., "Ink engineering of inkjet printing perovskite," *ACS Applied Materials & Interfaces*, vol. 12, no. 35, pp. 39082–39091, 2020.

[224] W. Gao, C. Chen, C. Ran et al., "A–site cation engineering of metal halide perovskites: version 3.0 of efficient tin-based lead-free perovskite solar cells," *Advanced Functional Materials*, vol. 30, no. 34, article 2000794, 2020.

[225] S. L. Hamukwaya, H. Hao, Z. Zhao et al., "A review of recent developments in preparation methods for large-area perovskite solar cells," *Coatings*, vol. 12, p. 252, 2022.

[226] N. K. Pendyala, S. Magdassi, and L. Etgar, "Fabrication of perovskite solar cells with digital control of transparency by inkjet printing," *ACS Applied Materials & Interfaces*, vol. 13, pp. 30524–30532, 2021.

[227] S. Ullah, J. Wang, P. Yang et al., "Evaporation deposition strategies for all-inorganic CsPb $(I_{1-x}Br_x)_3$ perovskite solar cells: recent advances and perspectives," *Solar RRL*, vol. 5, no. 8, article 2100172, 2021.

[228] W. Deng, F. Li, J. Li, M. Wang, Y. Hu, and M. Liu, "Anti-solvent free fabrication of FA-based perovskite at low temperature towards to high performance flexible perovskite solar cells," *Nano Energy*, vol. 70, article 104505, 2020.

[229] S. Lee, D. Jeong, C. Kim et al., "Eco-friendly polymer solar cells: advances in green-solvent processing and material design," *Acs Nano*, vol. 14, no. 11, pp. 14493–14527, 2020.

[230] M. Wang, C. Fei, M. A. Uddin, and J. Huang, "Influence of voids on the thermal and light stability of perovskite solar cells," *Science Advances*, vol. 8, no. 38, article eabo5977, 2022.

[231] J. Bing, S. Huang, and A. W. Ho-Baillie, "A review on halide perovskite film formation by sequential solution processing for solar cell applications," *Energy Technology*, vol. 8, no. 4, article 1901114, 2020.

[232] Z. Shi and A. H. Jayatissa, "Perovskites-based solar cells: a review of recent progress, materials and processing methods," *Materials*, vol. 11, no. 5, p. 729, 2018.

[233] D. Li, D. Zhang, K. S. Lim et al., "A review on scaling up perovskite solar cells," *Advanced Functional Materials*, vol. 31, no. 12, article 2008621, 2021.

[234] C. Ge, Y. Xue, L. Li, B. Tang, and H. Hu, "Recent progress in 2D/3D multidimensional metal halide perovskites solar cells," *Frontiers in Materials*, vol. 7, article 601179, 2020.

[235] P. Liu, N. Han, W. Wang, R. Ran, W. Zhou, and Z. Shao, "High-quality ruddlesden–popper perovskite film formation for high-performance perovskite solar cells," *Advanced Materials*, vol. 33, no. 10, article 2002582, 2021.

[236] E. K. Barimah, A. Boontan, D. P. Steenson, and G. Jose, "Infrared optical properties modulation of VO2 thin film fabricated by ultrafast pulsed laser deposition for thermochromic smart window applications," *Scientific Reports*, vol. 12, pp. 1–10, 2022.

[237] M. Xu, J. Yu, Y. Song, R. Ran, W. Wang, and Z. Shao, "Advances in ceramic thin films fabricated by pulsed laser deposition for intermediate-temperature solid oxide fuel cells," *Energy & Fuels*, vol. 34, no. 9, pp. 10568–10582, 2020.

[238] Z. Zhang, Q. Zhang, Q. Wang, H. Su, Y. Fu, and J. Xu, "Investigation on the material removal behavior of single crystal diamond by infrared nanosecond pulsed laser ablation," *Optics & Laser Technology*, vol. 126, article 106086, 2020.

[239] D. H. Blank, M. Dekkers, and G. Rijnders, "Pulsed laser deposition in Twente: from research tool towards industrial deposition," *Journal of Physics D: Applied Physics*, vol. 47, no. 3, article 034006, 2013.

[240] J. Chen, D. Jia, E. M. Johansson, A. Hagfeldt, and X. Zhang, "Emerging perovskite quantum dot solar cells: feasible approaches to boost performance," *Energy & Environmental Science*, vol. 14, no. 1, pp. 224–261, 2021.

[241] H. C. Wang, Z. Bao, H. Y. Tsai, A. C. Tang, and R. S. Liu, "Perovskite quantum dots and their application in light-emitting diodes," *Small*, vol. 14, no. 1, article 1702433, 2018.

[242] M. L. Meena, K. K. Gupta, S. Dutta et al., "Short review on the instability and potential solutions for perovskite quantum dots," *Current Research in Green and Sustainable Chemistry*, vol. 5, article 100321, 2022.

[243] M. Ilyas, A. Waris, A. U. Khan et al., "Biological synthesis of titanium dioxide nanoparticles from plants and microorganisms and their potential biomedical applications," *Inorganic Chemistry Communications*, vol. 133, article 108968, 2021.

[244] A. Haddout, A. Raidou, and M. Fahoume, "A review on the numerical modeling of CdS/CZTS-based solar cells," *Applied Physics A*, vol. 125, pp. 1–16, 2019.

[245] F. Belarbi, W. Rahal, D. Rached, and M. Adnane, "A comparative study of different buffer layers for CZTS solar cell using Scaps-1D simulation program," *Optik*, vol. 216, article 164743, 2020.

[246] S. H. Zyoud, A. H. Zyoud, N. M. Ahmed et al., "Numerical modeling of high conversion efficiency FTO/ZnO/CdS/CZTS/MO thin film-based solar cells: Using SCAPS-1D software," *Crystals*, vol. 11, no. 12, p. 1468, 2021.

[247] U. Mandadapu, S. V. Vedanayakam, K. Thyagarajan, and B. Babu, "Optimisation of high efficiency tin halide perovskite solar cells using SCAPS-1D," *International Journal of Simulation and Process Modelling*, vol. 13, no. 3, pp. 221–227, 2018.

[248] K. Ahmad, W. Raza, R. A. Khan, A. Alsalme, and H. Kim, "Numerical simulation of $NH_3(CH_2)_2NH_3MnCl_4$ based Pb-free perovskite solar cells via SCAPS-1D," *Nanomaterials*, vol. 12, no. 19, p. 3407, 2022.

[249] P. Kumari, U. Punia, D. Sharma, A. Srivastava, and S. K. Srivastava, "Enhanced photovoltaic performance of PEDOT: PSS/Si heterojunction Solar cell with ZnO BSF layer: a simulation study using SCAPS-1D," *Silicon*, vol. 15, no. 5, pp. 2099–2112, 2022.

[250] A. Houimi, S. Y. Gezgin, B. Mercimek, and H. Ş. Kılıç, "Numerical analysis of CZTS/n-Si solar cells using SCAPS-1D. A comparative study between experimental and calculated outputs," *Optical Materials*, vol. 121, article 111544, 2021.

[251] H. Bhattacharjee, A. Chakraborty, R. Ganguly, and M. Mitra, "Study on junction temperature management of White pcLED at high ambient temperature in industrial environment: an Indian perspective," in *2021 Devices for Integrated Circuit (DevIC)*, IEEE, 2021.

[252] Y. Park, C. Zechner, Y. Oh et al., "Dopant diffusion in Si, SiGe and Ge: TCAD model parameters determined with density functional theory," in *2017 IEEE International Electron Devices Meeting (IEDM)*, IEEE, 2017.

[253] W. Fichtner, D. J. Rose, and R. E. Bank, "Semiconductor device simulation," *SIAM Journal on Scientific and Statistical Computing*, vol. 4, no. 3, pp. 391–415, 1983.

[254] T. Binder, A. Hossinger, and S. Selberherr, "Rigorous integration of semiconductor process and device simulators," *IEEE Transactions on Computer-Aided Design of Integrated Circuits and Systems*, vol. 22, no. 9, pp. 1204–1214, 2003.

[255] M. Schwarz, V. Senz, A. Dannenberg et al., "Simulation methodology for active semiconductor devices in MEMS," in *2019 20th International Conference on Thermal, Mechanical and Multi-Physics Simulation and Experiments in Microelectronics and Microsystems (EuroSimE)*, pp. 1–4, Hannover, Germany, 2019.

[256] O. Karker, K. Zekentes, A. Bouchard et al., "Modelling and development of 4H-SiC nanowire/nanoribbon biosensing

FET structures," in *Materials Science Forum*, Trans Tech Publications Ltd., 2022.

[257] M. Hadjab, J.-M. Wagner, F. Bouzid et al., "A numerical optimization study of CdS and Mg0.125Zn0.875O buffer layers in CIGS-based solar cells using *wx*AMPS-1D package," *International Journal of Modelling and Simulation*, vol. 42, no. 2, pp. 179–191, 2022.

[258] J. Smucker and J. Gong, "A comparative study on the band diagrams and efficiencies of silicon and perovskite solar cells using wxAMPS and AMPS-1D," *Solar Energy*, vol. 228, pp. 187–199, 2021.

[259] Y. Liu, Y. Sun, and A. Rockett, "A new simulation software of solar cells—wxAMPS," *Solar Energy Materials and Solar Cells*, vol. 98, pp. 124–128, 2012.

[260] J. Fuhrmann, C. Guhlke, A. Linke, C. Merdon, and R. Müller, "Models and numerical methods for electrolyte flows," in *Topics in Applied Analysis and Optimisation*, pp. 183–209, Springer, 2019.

[261] Y. Liu, D. Heinzel, and A. Rockett, "A new solar cell simulator: WxAMPS," in *2011 37th IEEE Photovoltaic Specialists Conference*, Seattle, WA, USA, 2011.

[262] L. Zhang, Z. Wang, H. Zhou et al., "Synergistic coupling of $Li_{6.4}La_3Zr_{1.4}Ta_{0.6}O_{12}$ and fluoroethylene carbonate boosts electrochemical performances of poly(ethylene oxide)-based all-solid-state lithium batteries," *ChemElectroChem*, vol. 9, no. 17, article e202200641, 2022.

[263] H. Zhang, Z. Yu, C. Zhu, R. Yang, B. Yan, and G. Jiang, "Green or not? Environmental challenges from photovoltaic technology," *Environmental Pollution*, vol. 320, article 121066, 2023.

[264] T. A. Chowdhury, M. A. B. Zafar, M. S.-U. Islam, M. Shahinuzzaman, M. A. Islam, and M. U. Khandaker, "Stability of perovskite solar cells: issues and prospects," *RSC Advances*, vol. 13, no. 3, pp. 1787–1810, 2023.

[265] L. M. P. Caballero, F. N. D'Angelo, R. Tschentscher et al., "Developing the next generation of renewable energy technologies: an overview of low-TRL EU-funded research projects," *Open Research Europe*, vol. 3, no. 8, p. 8, 2023.

[266] M. Hasan Ali, A. T. M. Saiful Islam, M. D. Haque et al., "Touhidul Islam, Numerical analysis of $FeSi_2$ based solar cell with PEDOT:PSS hole transport layer. Materials today," *Communications*, vol. 34, article 105387, 2023.

[267] M. H. Ali et al., "Numerical analysis of FeSi2 based solar cell with PEDOT: PSS hole transport layer," *Materials Today Communications*, vol. 34, article 105387, 2023.

[268] D. T. Gangadharan and D. Ma, "Searching for stability at lower dimensions: current trends and future prospects of layered perovskite solar cells," *Energy & Environmental Science*, vol. 12, no. 10, pp. 2860–2889, 2019.

[269] G. Grancini, C. Roldán-Carmona, I. Zimmermann et al., "One-year stable perovskite solar cells by 2D/3D interface engineering," *Nature Communications*, vol. 8, pp. 1–8, 2017.

[270] C. Ortiz-Cervantes, P. Carmona-Monroy, and D. Solis-Ibarra, "Two-dimensional halide perovskites in solar cells: 2D or not 2D?," *ChemSusChem*, vol. 12, pp. 1560–1575, 2019.

[271] J. Hidalgo, A. F. Castro-Méndez, and J. P. Correa-Baena, "Imaging and mapping characterization tools for perovskite solar cells," *Advanced Energy Materials*, vol. 9, article 1900444, 2019.

[272] G. Nazir, S. Y. Lee, J. H. Lee et al., "Stabilization of perovskite solar cells: recent developments and future perspectives," *Advanced Materials*, vol. 34, no. 50, article 2204380, 2022.

[273] J. Bing, L. G. Caro, H. P. Talathi, N. L. Chang, D. R. Mckenzie, and A. W. Ho-Baillie, "Perovskite solar cells for building integrated photovoltaics—glazing applications," *Joule*, vol. 6, no. 7, 2022.

[274] Y. Sun, R. Ma, Y. Kan et al., "Simultaneously enhanced efficiency and mechanical durability in ternary solar cells enabled by low-cost incompletely separated fullerenes," *Macromolecular Rapid Communications*, vol. 43, no. 22, article 2200139, 2022.